Supporting information for:

Aromatic and aliphatic hydrocarbon hydroxylation via a formally Ni^{IV}=O oxidant

Philipp Heim,[1] Robert Gericke,[1,2] Giuseppe Spedalotto,[1] Marta Lovisari,[1] Erik R. Farquhar,[3] Aidan R. McDonald*[1]

[1] School of Chemistry and CRANN/AMBER Nanoscience Institute, Trinity College Dublin, The University of Dublin, College Green, Dublin 2, Ireland

[2] Current address: Helmholtz-Zentrum Dresden-Rossendorf e.V., Institute of Resource Ecology, Bautzner Landstraße 400, 01328 Dresden, Germany

[3] Center for Synchrotron Biosciences, National Synchrotron Light Source II, Brookhaven, National Laboratory Case Western Reserve University, Upton, NY 11973 (USA)

E-mail: aidan.mcdonald@tcd.ie

Methods:

NMR spectra were measured on an Agilent MR 400 MHz NMR spectrometer. Fourier transform infra-red spectra were collected on a Perkin Elmer Spectrum 100 Fourier transform infra-red. Electrospray ionisation mass spectrometry was carried out on a Micromass Time of Flight (ToF), interfaced with a Waters 2690 HPLC. UV-Vis electronic absorption spectra were recorded using an Agilent 8453 diode array spectrophotometer (190 - 1100 nm range), attached to a Unisoku Scientific Instrument cryostat using liquid nitrogen as coolant.

Electrochemical analysis: Cyclic Voltammetry (CV) was conducted on a MS Instrument 600E electrochemical analyser, using glassy carbon as the working electrode, Pt wire as the counter electrode, and an Ag/Ag^{+} (0.01 M in CH_3CN) reference electrode. All CVs were referenced against the ferrocene/ferrocenium (Fc/Fc^{+}) redox couple. Cyclic Voltammetry (CV) experiments were conducted on 1.0 mM solutions in CH_3CN at room temperature. $[^{n}Bu_4N][NPF_6]$ (0.10 M) was used as the supporting electrolyte.

Electron paramagnetic resonance: EPR spectra of frozen solutions of **2** and $[Ni^{III}(m\text{-}CBA)(L^{Ph})]^{-}$ were acquired on a Bruker EMX X-band EPR, equipped with an Oxford Instruments CE 5396, ESR9 Continuous Flow Cryostat, a precision Temperature Controller and an Oxford Instruments TTL20.0/13 Transfer Tube. EPR samples were prepared by freezing the EPR tubes containing the analyte solutions, previously prepared at the UV-Vis spectrophotomer, in liquid nitrogen. EPR spectra of **2** and **2[*m*-CBA]** were recorded at 77 K, 9.2 GHz, 2.01 mW microwave power, with a 120 mT field sweep in 84 s, and 0.3 mT field modulation amplitude. Integration, simulation, and fitting were performed with Matlab and the easySpin computational package.[1] The oxidation yield of the samples was calculated by quantification of the concentration of spins in the samples. This was obtained by comparison

of the double integral of the signals to that of a frozen solution of (2,2,6,6-tetramethyl-piperidin-1-yl)oxyl (TEMPO, 5 mM), measured under the same conditions.

Gas Chromatography Flame-Ionization detection (GC-FID) analysis: Gas chromatographic studies were carried out on a ThermoFisher TRACE^{TM} 1300 Gas Chromatograph, equipped with a Flame Ionization detector. Hydrogen gas was provided by a Parker Hydrogen Gas generator 20H-MD. Air was provided by Parker Zero Air Generator UHP-10ZA-S. The column used was a ThermoFisher TraceGOLD TG-1MS GC column. The instrument method for the *m*-CPBA decay products was based on a temperature ramp (1 min. at 60 °C, 10 °C/min until 160 °C. Hold 160 °C for 1 min.), with splitless injections of 1 μL each. The retention time for the products were noted as follows within the error of ± 0.2 minutes: chlorobenzene (3.1 minutes), aniline (4.5) 1,3-dichlorobenzene (5.1), 3-chlorophenol (7.6), 3-chlorobenzoic acid (9.8). The instrument method for cyclohexene oxidation products was based on a temperature ramp (2 min. at 40 °C, 8 °C/min. for 10.5 min., hold at 125 °C for 2 min.) with splitless injections of 1 μL each. The retention time for cyclohexene oxidation products were noted as follows: 1,2-eopxycyclohexane (7.2), cyclohexen-2-ol (7.7) and cyclohexen-2-one (8.4). The quantification of each was based on a calibration curve of a pure standard. The yields were calculated based on the average of triplicate measurements of a reaction mixture. The instrument method for 2,6-DTBQ was based on a temperature ramp (2 min. at 75 °C, 10 °C/min. to 200 °C, 2 min. at 200 °C) with splitless injections of 1 μL each. The retention time for 2,6-DTBQ was noted as 12.3 ± 0.2 minutes. The quantification of 2,6-DTBQ was based on a calibration curve of a pure standard. The yields were calculated based on the average of triplicate measurements of a reaction mixture.

XAS data collection and analysis: XAS samples were prepared by transferring 5.0 mM solutions containing **2** (prepared as described below) from a quartz cuvette to a pre-chilled Delrin® XAS sample holder (~0.2 mL) using a pre-cooled Pasteur pipette. The sample holder containing **2** was slowly allowed to solidify in liquid N_2, avoiding the formation of gas bubbles during the freezing process. The frozen solutions were transferred into a storage dewar until measurement.

The Ni-K-edge X-ray absorption data were collected on beam line 7-3 at SSRL (*Stanford Synchrotron Radiation Lightsource*, SLAC National Accelerator Lab, Menlo Park, CA, USA). Data were collected with the storage ring operating at ca. 3 GeV and 500 mA, using a LN_2 cooled Si (220), ϕ = 0˚ & 90˚ double-crystal monochromator, calibrated by using the first inflection point of a Ni foil (8333.0 eV). The monochromator was detuned by ~30% for higher harmonic rejection. The fluoresce detector used was a Canberra 30-element Ge solid state detector, cooled with LN_2. All the measurements were performed at ambient pressure at ~17 K, gained by an Oxford Helium cryostat, cooled by closed-cycle He gas loop. The parameters used for the scans were the following: 10 eV steps/1 second integration time in the pre-edge region, 0.3 eV steps/2 second integration time in the edge, and 0.05k steps in the EXAFS, with integration time increasing in a k^2-weighted fashion from 2 to 9 seconds over the energy range (k_{max} = 15.1k). The total detector counts were in the range between 20k-35k, well within the linear range of the detector electronics. Each sample was monitored for radiation damage, using different spots where required to ensure a perfect reproducibility of the data.

Elaboration of the XAS data, including averaging, background removal and normalization, was performed using Athena.[2] Edge energies were determined as main peak in first derivative and

zero-crossings in the second derivative. EXAFS analysis was carried out using Artemis,[2] which incorporates the IFEFFIT fitting engine and FEFF6 for ab initio EXAFS phase and amplitude parameters. Crystal structures (either as-is or modified slightly to test different structural models) were used for FEFF6 input to identify significant paths.

Computational Results: The geometry optimizations were carried out with ORCA 5.0.2 or 5.0.3[3] using DFT unrestricted PBE0 functional with relativistically recontracted Karlsruhe basis set ZORA-def2-TZVPP[4, 5] for all atoms, scalar relativistic ZORA Hamiltonian[6, 7], atom-pairwise dispersion correction with the Becke-Johnson damping scheme (D3BJ)[8, 9] and COSMO solvation (CH_2Cl_2). Calculations were started from the molecular structure of **1[OAc]** obtained by single-crystal X-ray diffraction analysis. Numerical frequency calculations were performed to prove that the minimum was obtained after geometry optimization. Gibbs free energies are given at 293.15 K, if not stated otherwise. The g-tensor and the hyperfine coupling constant were calculated with the EPR/NMR module implemented in ORCA 5.0.2. The spin-density and Wiberg bond order were calculated using Multiwfn.[10]

Materials

All reactions with air sensitive materials were carried out in an inert atmosphere glovebox or manipulated under a N_2 or Ar atmosphere using Schlenk line techniques. All reagents were purchased from commercial sources and were used as received. Peroxybenzoic acid, (PBA), bis(3-chlorobenzoyl)peroxide and 2,2',2''-nitrilo-*tris*-(N-phenyl)acetamide (H_3L^{Ph}) were synthesized flowing literature procedures.[11-13] H_2O_2 was prepared according to a previous report.[14] N,N-dimethylformamide (DMF) was purchased and stored under an inert atmosphere in a Schlenk tube containing 3 Å molecular sieves. Dry CH_3CN and diethylether (Et_2O) were dispensed from a MBRAUN Solvent Purification System (SPS-5) and deoxygenated by purging a flow of nitrogen through the solution. [$^nBu_4N$][NPF_6] was recrystallised three times from 3:1 EtOH/water mixture and dried *in vacuo* for 2 days prior to use. 2,4,6-*tris*-*tert*-butylphenol (TTBP) was recrystallized twice from hexane and dried *in vacuo* prior to use. Commercially available 3-chloroperoxybenzoic acid (*m*-CPBA) (≤77%) was purified by washing with a pH = 7.5 buffer solution. A purity of 86% was determined *via* iodometric titration. Water sensitive products were stored in an inert atmosphere glovebox or stored under vacuum in a desiccator containing $CaCl_2$ as drying agent.

CAUTION: Peroxyacids are potentially explosive once obtained as a dry powder. Compounds were stored at -20 °C and when used, were never heated above 40 °C. No problems were encountered during this research.

Synthesis of ^{18}O-labelled 3-chloroperoxybenzoic acid (^{18}O-m-CPBA)

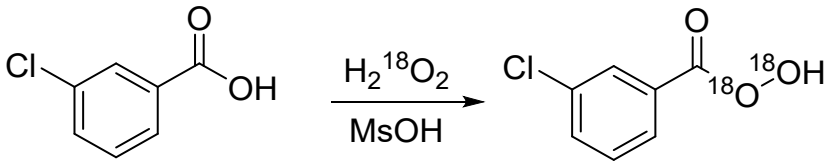

The title compound was synthesized from an adapted procedure.[11] 3-chlorobenzoic acid (177.4 mg, 1.13 mmol) was added to a screw-cap test tube, and to it was added methane sulfonic acid (1.1 mL) and CH_2Cl_2 (0.8 mL). Previously prepared $H_2{}^{18}O_2$ (~30% w/v, 0.28 mL, 2.44 mmol)[15] was added dropwise over the course of 5 minutes with vigorous stirring. The yellow mixture was heated to 40 °C and stirred for 4.5 hours, forming a pale yellow solution. The solution was allowed to cool to room temperature, and then was added to a saturated $(NH_4)_2SO_4$ solution (10 mL) in ice, causing the precipitation of a white solid. The solid was re-dissolved in CH_2Cl_2 and the aqueous layer was extracted twice with CH_2Cl_2 (2 x 5 mL). The combined organic extracts were washed with saturated $(NH_4)_2SO_4$ solution (2 x 5 mL) and twice with phosphate buffer solution (pH = 7.5, 2 x 10 mL). The organic layer was dried over $MgSO_4$, and volatiles were evaporated under a flow of N_2, leaving behind a white powder. Yield = 100 mg, 50%. Iodometric titration of liberated I_2 against $Na_2S_2O_3$•$5H_2O$ indicated 96% active oxygen.

Preparation of [$Ni^{III}(OL^{Ph})$] **(2)**

1[OAc] (67.9 mg, 0.10 mmol) was dissolved in dry CH_3CN (10 mL) to make a 10.0 mM stock solution which was further diluted to a 0.50 mM solution with CH_3CN. 2 mL of **1[OAc]** (0.50 mM) was transferred into a quartz cuvette and sealed with a septum. *m*-CPBA (88%) (19.6 mg, 0.10 mmol) was dissolved in CH_2Cl_2 (5 mL) to make a 0.020 M solution. The cuvette containing **1[OAc]** was placed into the cryostat/UV-Vis spectrometer and was cooled to -40

°C. *m*-CPBA (88%) (0.020 M, 50 µL, 1.0 equiv.) was added to **1[OAc]** at -40 °C under continuous stirring, causing a gradual colour change from pale green to dark green.

Reactivity experiments and rate constant determination:

A solution of **2** was prepared as described above. Substrates were added as concentrated solutions (0.1 – 2.0 M) in CH_2Cl_2 to a stirred solution of **2** at -40 °C in CH_3CN. The progress of the reaction was monitored *via* UV-Vis spectroscopy, by observing the disappearance of the λ = 390 nm feature for **2**. Reaction rate constants were determined by using a minimum of 10.0 equivalents of substrate with respect to [Ni], to ensure *pseudo*-first order conditions. Each measurement of k_{obs} was repeated three times to estimate a standard deviation to within 10% (indicated by error bars). Second order rate constants were determined by plotting the dependence of the *pseudo*-first order rate constants (k_{obs}) *versus* the concentration of the substrates. The value of k_2 was determined from the slope of the obtained line.

Quantification of m-CPBA decay products:

A solution of **1[OAc]** (10 mM, 2 mL) was treated with *m*-CPBA (1.0 equiv.) in CH_3CN at -40 °C. The solution was allowed to stir at -40 °C for 1 hour, before being warmed to room temperature. The reaction mixture was further allowed to stir for 12 hours. The brick red mixture was treated with HCl (1.0 N, 2 mL) and the organic products were extracted with CH_2Cl_2 (3 x 2 mL). The organic phase was dried over $MgSO_4$, filtered and the solvent was removed under reduced pressure to yield an orange residue. 1,3,5-trimethylbenzene (10 µL, 0.073 mmol) was added as an internal standard, and the combined mixture was taken up in $CDCl_3$ for ^1H NMR analysis.

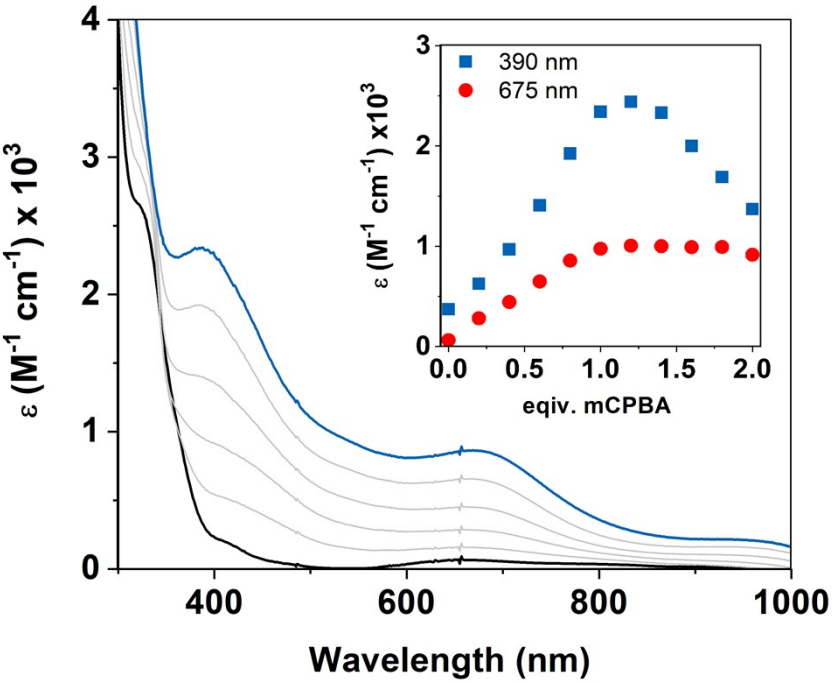

Figure S1. Electronic absorption spectrum of **1[OAc]** (black trace), 0.2 equiv. incremental additions of *m*-CPBA to **1[OAc]** (grey traces) to yield **2** (blue trace) in CH_3CN at -40 °C.

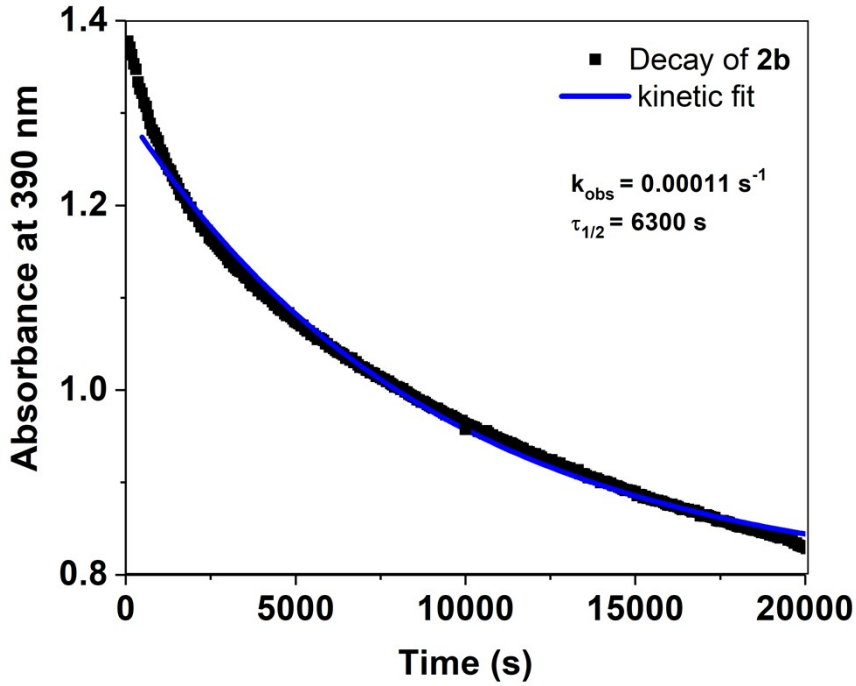

Figure S2. Trace monitoring the natural decay of **2** (λ = 390 nm), in CH_3CN at -40 °C.

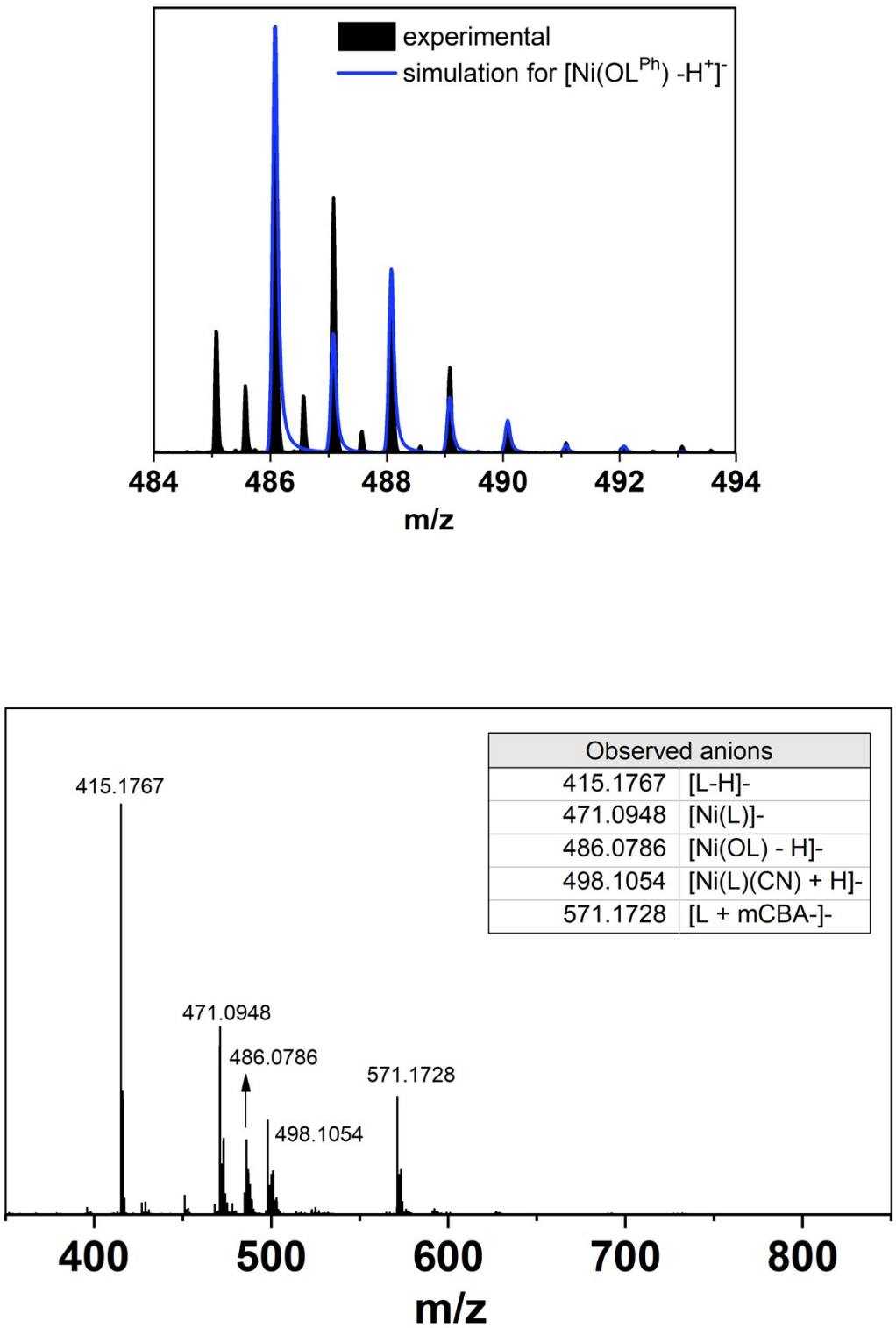

Figure S3. Top: Negative mode ESI-MS spectrum obtained for **2**. Black signal = experimental result, displaying m/Z = 486.0786. Blue trace = simulation for $[Ni(L^{Ph}) +(O) – (H)]^-$, calc. m/Z for $C_{24}H_{20}N_4NiO_4$ = 486.0837. Bottom: entire spectrum.

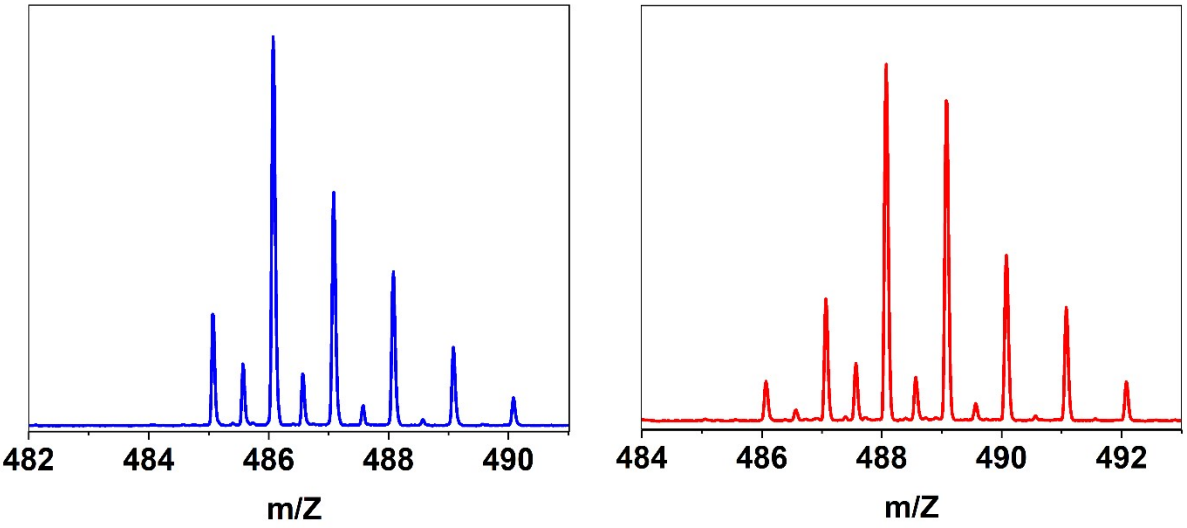

Figure S4. Negative mode ESI-MS spectra of reactions of **1[OAc]** with 1.0 equiv. ^{16}O-*m*-CPBA (left) and 1.0 equiv. ^{18}O-*m*-CPBA (right) at -40 °C in CH_3CN.

Table S1. XANES pre-edge peak fitting parameters. The values in parentheses correspond to uncertainty in the final digit for each parameter, taken as the standard deviation determined from the three separate fits conducted on each sample.

	$E_{pre\text{-}edge}$ (eV)[a]	Height	FWHM	Area[b]
1[OAc]	8332.65(1)	0.0379(1)	1.86(2)	9.3(1)
2	8332.95(1)	0.0220(2)	1.77(4)	5.1(2)

[a] The pre-edge energies correspond to the centre of the pseudo Voigt functions. [b] Areas are multiplied by 10^2 for convenience.

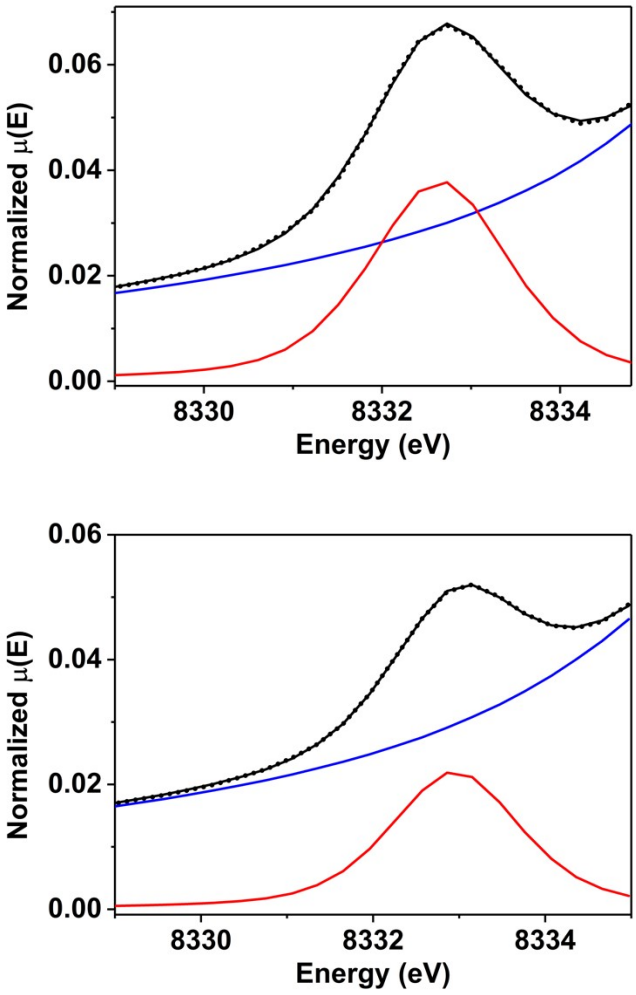

Figure S5. Representative pre-edge peak fits of **1[OAc] (top)** and **2 (bottom)**. Experimental data (dotted line), background function (blue line), component pre-edge functions (red lines), sum of the background + component functions (black line).

Table S2. EXAFS Fitting of the data for **1[OAc]**. Significant fits are highlighted in bold. Fitting range was k = 2-13.0 $Å^{-1}$ with back transform ranges of 1.15-1.92 Å for fits 1-3, 1.15-2.82 Å for fits 4-25. r is in units of Å; σ^2 is in units of 10^{-3} Å; ΔE_0 is in units of eV; R represents the fractional mis-fit of the data, while χ^2 is the χ^2 fitting metric normalized by the number of independent data points in a given fit.

	Ni-N/O			Ni-N/O			Ni···C			Ni···C					
fit	n	r	σ^2	n	r	σ^2	n	r	σ^2	n	r	σ^2	ΔE_0	χ^2	R
1	5	2.05	4.88										4.68	97.597	0.0114
2	6	2.05	6.28										4.20	91.942	0.0107
3	7	2.05	7.63										3.76	183.481	0.0214
4	5	2.05	4.61										4.65	236.050	0.0893
5	6	2.05	5.93										4.15	236.450	0.0894
6	5	2.06	4.26	1	2.23	9.73							6.35	280.282	0.0805
7	5	2.06	4.30	2	2.25	15.11							7.20	262.522	0.0754
8	5	2.07	3.58	1	2.25	1.21	1	2.49	1.19				8.47	366.302	0.0720
9	5	2.07	3.25	1	2.23	0.26	2	2.46	5.71				9.45	363.073	0.0714
10	5	2.07	3.05	1	2.22	0.02	3	2.44	8.75				10.23	353.038	0.0694
13	5	2.06	4.45	1	1.92	9.34	1	2.35	14.10	3	2.85	2.17	4.07	69.230	0.0073
14	5	2.05	4.84	1	2.17	35.36	1	2.48	14.67	4	2.86	3.95	5.14	78.921	0.0084
15	5	2.05	4.76	1	2.30	38.48	1	2.55	11.50	5	2.86	5.39	4.80	92.637	0.0098
16	**5**	**2.05**	**4.97**	**1**	**2.40**	**7.15**	**1**	**2.61**	**0.95**	**6**	**2.84**	**6.04**	**3.71**	**93.951**	**0.0099**
17	5	2.05	5.11	1	2.39	4.32	1	2.59	-0.89	7	2.83	7.66	3.32	93.228	0.0099
18	5	2.05	5.22	1	2.39	2.63	1	2.58	-1.94	8	2.83	9.25	3.00	94.154	0.0100
19	6	2.06	5.81				1	2.35	8.42				5.45	291.452	0.0838
20	6	2.06	5.71				2	2.35	12.16				6.30	280.152	0.0805
21	6	2.06	6.11				1	2.39	7.48	3	2.86	1.98	5.15	50.418	0.0099
22	6	2.05	6.10				1	2.42	9.50	4	2.86	3.80	4.89	62.431	0.0123
23	6	2.05	6.11				1	2.46	11.58	5	2.86	5.48	4.51	83.369	0.0164
24	6	2.05	6.12				1	2.49	10.75	6	2.86	7.07	4.24	108.947	0.0214
25	6	2.05	6.13				1	2.51	8.86	7	2.86	8.87	4.03	137.000	0.0270

Table S3. EXAFS Fitting of the data for **2**. Significant fits are highlighted in bold. Fitting range was k = 2-14.0 $Å^{-1}$ with back transform ranges of 1.15-1.97 Å for fits 1-10, 1.15-2.82 Å for fits 11-31. r is in units of Å; σ^2 is in units of 10^{-3} Å; ΔE_0 is in units of eV; R represents the fractional mis-fit of the data, while χ^2 is the χ^2 fitting metric normalized by the number of independent data points in a given fit.

	Ni-N/O			Ni-N/O			Ni···C			Ni···C			Ni···C					
fit	n	r	σ^2	n	r	σ^2	n	r	σ^2	n	r	σ^2	n	r	σ^2	ΔE_0	χ^2	R
1	4	2.08	14.39													12.34	1339.063	0.2651
2	5	2.07	16.91													11.01	1121.690	0.1110
3	6	2.07	19.05													9.95	971.775	0.1924
4				4	2.11	12.03										12.34	1427.403	0.2825
5				5	2.10	14.44										11.67	1204.612	0.2384
6				6	2.09	16.58										10.68	1044.897	0.2068
7	1	1.87	1.26	4	2.07	6.54										5.61	1136.948	0.0784
8	2	2.07	1.74	3	1.92	4.79										2.54	1171.830	0.0808
9	3	1.91	7.63	2	2.10	1.73										2.43	1458.545	0.1005
10	4	2.12	15.50	1	0.82	3.63										15.24	2686.015	0.1851
11	2	2.07	1.72	3	1.93	4.88										3.07	469.178	0.1731
12	1	1.52	9.43	4	2.16	15.22										16.90	646.359	0.2384
13	2	2.07	1.55	3	1.92	4.63	1	2.74	-0.81							2.81	279.809	0.0743
14	2	2.07	1.72	3	1.92	4.75	2	2.75	2.12							2.59	175.980	0.0467
15	2	2.07	1.84	3	1.92	4.82	3	2.75	4.28							2.44	120.323	0.0319
16	2	2.07	1.92	3	1.92	4.87	4	2.75	6.17							2.32	91.528	0.0243
17	2	2.06	1.98	3	1.91	4.89	5	2.76	7.98							2.19	79.180	0.0210
18	2	2.06	2.02	3	1.91	4.90	6	2.76	9.76							2.06	77.017	0.0204
19	2	2.06	2.06	3	1.91	4.90	7	2.76	11.55							1.92	80.948	0.0215
20	2	2.06	2.08	3	1.91	4.88	8	2.76	13.35							1.77	88.237	0.0234
21	2	2.07	1.59	3	1.92	4.72	2	2.74	-0.04	1	2.87	-0.53				3.10	163.869	0.0266
22	2	2.07	1.71	3	1.92	4.83	2	2.85	3.80	2	2.73	1.00				3.11	122.512	0.0199
23	2	2.07	1.78	3	1.92	4.90	2	2.88	4.51	3	2.74	2.75				3.14	101.899	0.0165
24	2	2.07	1.84	3	1.92	4.95	2	2.91	5.17	4	2.75	4.40				3.14	98.413	0.0160
25	2	2.06	2.03	3	1.91	4.60	2	2.57	10.68	5	2.75	6.44				0.44	105.927	0.0172
26	2	2.05	2.03	3	1.90	4.45	2	2.52	7.05	6	2.74	7.13				-0.37	83.432	0.0135
27	2	2.06	1.51	3	1.91	4.29	2	2.62	5.34	3	2.75	-0.12	1	2.89	-2.85	1.47	109.116	0.0064
28	2	2.06	1.52	3	1.91	4.22	2	2.58	4.41	3	2.73	-0.42	2	2.86	-0.18	0.98	69.771	0.0041
29	**2**	**2.06**	**1.57**	**3**	**1.90**	**4.19**	**2**	**2.56**	**3.77**	**3**	**2.71**	**0.12**	**3**	**2.84**	**2.31**	**0.57**	**47.814**	**0.0028**
30	2	2.06	1.56	3	1.91	4.24	2	2.58	5.30	4	2.75	1.47	1	2.89	-0.21	0.95	76.783	0.0045
31	2	2.06	1.59	3	1.90	4.20	2	2.55	4.16	4	2.72	1.20	2	2.86	0.62	0.54	50.389	0.0030

Table S4. Comparison of selected bond length between XRD data (average) and EXAFS Fit for **1[OAc]** and DFT and EXAFS fits for **2**.

XRD of **1[OAc]**		EXAFS Fit of **1[OAc]**		DFT of **2** (see Figure S8)		EXAFS Fit of **2**	
Ni-N	2.06 Å	Ni-N	2.05 Å	Ni1-O3	1.83 Å	Ni-N/O	1.90
Ni_O_{acet}	2.32 Å	Ni-O_{acet}	2.40 Å	Ni1-N11	1.84 Å		
Ni···C_{acet}	2.51 Å	Ni···C_{acet}	2.61 Å	Ni1-N6	1.91 Å		
Ni···C_{NTA}	2.87 Å	Ni···C_{NTA}	2.84 Å	Ni1-N7	1.92 Å	Ni-N/O	2.06
				Ni1-N4	2.02 Å		

Table S5. Significant data from Ni K-edge X-ray absorption spectroscopy analysis of complexes **1[OAc]** and **2**.

	E_{edge}[a]	$E_{pre\text{-}edge}$[a]	$Area_{pre\text{-}edge}$[b]	EXAFS Fit	
				1st [c]	2nd [c]
1[OAc]	8343.4	8332.7	9.4	5 N/O @ 2.05	1 N/O @ 2.40 1 C @ 2.61 6 C @ 2.84
2	8344.4	8333.1	5.2	2 N/O @ 1.2.06 3 N/O @ 1.90	C @ 2.56 3 @ 2.71 3 @ 2.84

[a] Energy values reported in eV. [b] Areas multiplied by 100 for convenience. [c] Distances reported in Å.

Atomic coordinates and total energies:

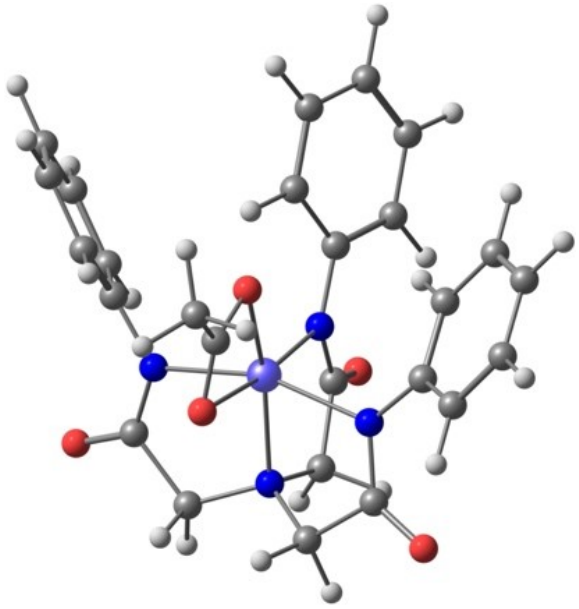

Figure S6. Optimized molecular structure of **1[OAc]** (S = 1). Final single point energy: -3128.334439676697 a.u.; final Gibbs free energy: -3127.93033024 a.u.

Table S6. Atomic coordinates for optimized structure of **1[OAc]** (S = 1).

Ni	0.000000000	0.000000000	2.067078582
O	3.626723604	0.156771974	0.218685343
O	-0.666374369	-0.122621199	4.060635487
O	-2.242901413	0.006290974	2.535642188
N	2.058886996	0.000000000	1.923702437
O	-1.112548854	-3.417789048	0.058523254
N	-0.227550496	-2.049142489	1.713440255
N	0.000000000	0.000000000	0.000000000
C	2.473109011	0.011762929	0.661832880
C	0.969023324	-2.953809254	3.581076792
H	1.686710779	-2.154775609	3.446541298
N	0.001221840	2.071496716	1.777165167
C	2.951078956	0.095374918	2.985969274
O	-0.037359453	3.590122200	0.030544610
C	-1.044169380	-4.057624805	2.889265746
H	-1.885602901	-4.137942041	2.216176762
C	-1.884840972	-0.125406754	3.728645752
C	4.297885444	-0.301918302	2.938953605
H	4.705906009	-0.665103974	2.008408882
C	3.269298482	0.632507406	5.335863711
H	2.850396868	0.999975462	6.266664209
C	-0.110621086	-3.030806111	2.691889540
C	2.459973494	0.557024501	4.216168457
H	1.420794302	0.849247899	4.277684780
C	0.181099670	-4.873331588	4.804934522

H	0.291071407	-5.581632470	5.617932562
C	-0.730575616	-2.325460662	0.517902240
C	4.601895929	0.241838707	5.275488634
H	5.237154757	0.300402487	6.151740025
C	1.113574460	-3.859140983	4.617932018
H	1.960472913	-3.767727262	5.289679771
C	-0.896127067	-4.960240398	3.932668061
H	-1.637626163	-5.741188082	4.066188356
C	1.393798341	-0.240538958	-0.386141621
H	1.651057190	0.342214954	-1.275142228
H	1.500332594	-1.294249155	-0.658475255
C	5.100671719	-0.228248428	4.068243598
H	6.135525836	-0.547478009	3.999053218
C	0.443401317	2.989883443	2.725462548
C	-0.251286329	3.140132273	3.927995925
H	-1.165389828	2.578317154	4.070644371
C	0.227875314	3.969719776	4.930981207
H	-0.327603578	4.060961197	5.858233909
C	1.411772055	4.674418913	4.758061779
H	1.790472933	5.316767739	5.544458785
C	2.106823082	4.540076495	3.561101410
H	3.037214519	5.077558621	3.411788539
C	1.630761921	3.712529878	2.558501463
H	2.185995340	3.596662252	1.636344312
C	-0.115117051	2.443906574	0.511828123
C	-2.923464176	-0.326339860	4.801842048
H	-3.163242372	-1.391897897	4.851658046
H	-3.838378729	0.212664786	4.558583324
H	-2.547213060	-0.016270868	5.775422513
C	-0.866164247	-1.108430323	-0.390514790
H	-0.689111433	-1.422918169	-1.424985120
H	-1.904565553	-0.777508036	-0.317242497
C	-0.483116247	1.306988371	-0.434908869
H	-1.574191571	1.275346207	-0.478438868
H	-0.120429707	1.558103012	-1.436777516

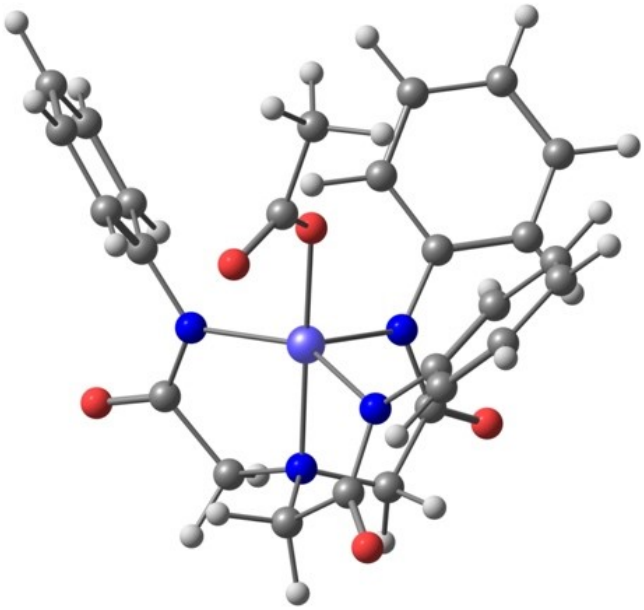

Figure S7. Optimized molecular structure of **1[OAc]** (S = 0). Final single point energy: -3128.314807471359 a.u.; final Gibbs free energy: -3127.91063849 a.u.

Table S7. Atomic coordinates for optimized structure of **1[OAc]** (S = 0).

Ni	0.000000000	0.000000000	0.000000000
O	-1.387643199	-3.241426978	-2.233680244
O	0.000000000	0.000000000	1.944604118
O	0.074041584	2.221038977	2.204942571
N	-0.501997110	-2.055999506	-0.439056024
O	-2.629395246	2.574292588	-1.617159180
N	-1.761877885	0.951878598	-0.195375294
N	-0.083752827	0.109727916	-2.005089399
C	-0.971167310	-2.212503912	-1.667444821
C	-3.063461982	-0.225848191	1.423286592
H	-2.488878923	-1.105386961	1.160113482
N	1.979373125	0.000000000	-0.274576210
C	-0.473649089	-3.102600285	0.471358701
O	3.543641669	-0.008067066	-1.976391280
C	-3.505339067	2.112913451	1.114575738
H	-3.295740856	3.047832537	0.616544055
C	-0.078375078	1.069836007	2.630909249
C	-1.454726123	-4.101719886	0.562057509
H	-2.266023999	-4.105454784	-0.151842843
C	0.626648181	-4.099898260	2.393335797
H	1.443814845	-4.085346265	3.106712284
C	-2.778026369	0.971890950	0.755642238
C	0.562243708	-3.122884255	1.415516177
H	1.308722578	-2.340540087	1.370113848
C	-4.761101748	0.851117217	2.748221053
H	-5.525377112	0.806811036	3.515384842
C	-1.792468416	1.722679174	-1.281143523
C	-0.349504159	-5.087111749	2.471469981
H	-0.303029945	-5.850578525	3.239319712
C	-4.040463875	-0.286296622	2.401097562

H	-4.238092161	-1.229251383	2.899255939
C	-4.481853570	2.045832838	2.098414022
H	-5.028380368	2.944878160	2.362850126
C	-1.021220671	-0.917588069	-2.470027594
H	-0.858584201	-1.143710800	-3.527742156
H	-2.037234736	-0.530630904	-2.368855176
C	-1.388495918	-5.074318633	1.549297780
H	-2.164273699	-5.831397976	1.599125334
C	2.947206159	-0.112553221	0.732353395
C	3.045737463	0.861052436	1.724814995
H	2.380278597	1.714203236	1.683135463
C	3.951956332	0.723168398	2.765637213
H	4.004988506	1.490054473	3.530722604
C	4.781444077	-0.388305107	2.836118238
H	5.486641228	-0.497290838	3.651808186
C	4.691953695	-1.362569291	1.849075382
H	5.329366111	-2.238998484	1.892143479
C	3.785978885	-1.227520835	0.808985845
H	3.712187042	-1.992608672	0.045873523
C	2.380522145	-0.015288666	-1.541046710
C	-0.410535837	0.845795658	4.092499853
H	-1.478534564	0.624335763	4.169352830
H	-0.191791840	1.731628263	4.686516311
H	0.132581656	-0.015044075	4.483617259
C	-0.617697006	1.454500454	-2.217153226
H	-0.943629878	1.606359342	-3.252059432
H	0.172337533	2.179464870	-2.002800094
C	1.257100800	-0.085063816	-2.560263532
H	1.457788359	0.624488751	-3.367428681
H	1.314336015	-1.084668734	-2.996934933

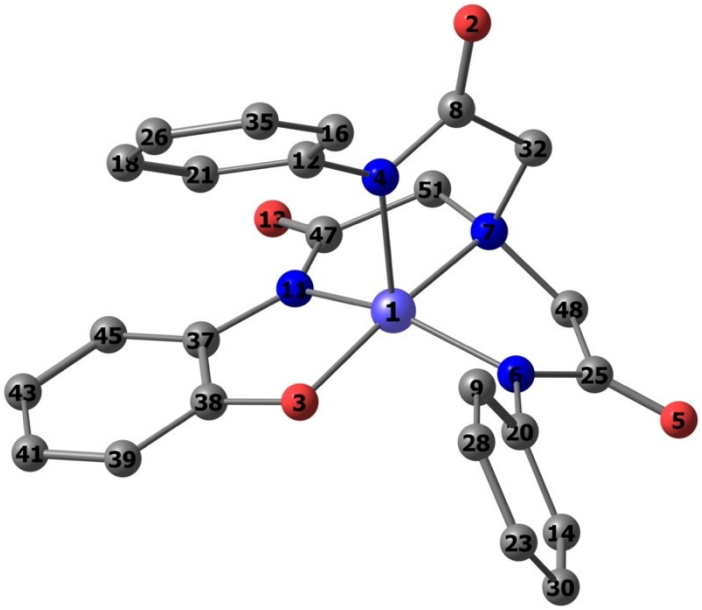

Figure S8. Geometry optimized molecular structure of **2** (S = ½). The coordinate system displays the g-tensor orientation. H atoms have been omitted for clarity; Final single point energy: -2974.293021839146 a.u.; final Gibbs free energy: -2973.93825510 a.u.

Table S8. Atomic coordinates for optimized structure of **2** (S = ½).

Ni	0.000000000	0.000000000	0.000000000
O	-0.902421148	-1.534113871	3.637539550
O	0.533442575	1.710103393	-0.381375343
N	-0.055237559	-0.116647331	2.018720181
O	-3.405734143	-0.959449182	-1.681946863
N	-1.831821242	0.234724884	-0.474411990
N	-0.446713472	-1.861007002	0.076766590
C	-0.668409304	-1.203976556	2.470152431
C	-2.462514018	2.192979234	0.766325576
H	-1.898921996	1.800149416	1.602135406
N	1.737168759	-0.494810581	-0.331113064
C	0.369168573	0.894163293	2.886553913
O	3.069717583	-2.327812776	-0.727961088
C	-3.231765656	1.970385165	-1.498567240
H	-3.278188702	1.409124778	-2.420720430
C	-0.482621632	1.449358615	3.845552283
H	-1.482848682	1.051348894	3.956088125
C	2.079444989	2.465396636	3.555426156
H	3.082620466	2.857424181	3.432851378
C	-2.524773949	1.450712428	-0.412555730
C	1.656877732	1.413967620	2.757364313
H	2.322986048	0.987755711	2.018356483
C	-3.809882431	3.928767594	-0.214564160

H	-4.308298011	4.887785043	-0.139439390
C	-2.325641532	-0.842887753	-1.108071213
C	1.227000742	3.015281846	4.503541477
H	1.556491632	3.838697400	5.125864552
C	-3.097812730	3.419696086	0.863614002
H	-3.033669449	3.980918452	1.788846053
C	-3.869764371	3.196949014	-1.393021862
H	-4.414350975	3.586493767	-2.245678089
C	-1.148413078	-2.111113971	1.351039478
H	-1.040764230	-3.157065017	1.640544693
H	-2.211123854	-1.908885255	1.208584984
C	-0.054397796	2.497518780	4.644540022
H	-0.731202851	2.917297760	5.380161764
C	2.581616686	0.586905388	-0.572647378
C	1.846704720	1.788111928	-0.582419146
C	2.508089239	2.993858633	-0.792208687
H	1.939302256	3.916311116	-0.796137373
C	3.885248520	2.993635653	-0.981036095
H	4.399442279	3.934880627	-1.138507118
C	4.606430897	1.806008611	-0.965750389
H	5.679745064	1.820161269	-1.111949074
C	3.957826777	0.591830632	-0.759450739
H	4.504914113	-0.339710910	-0.743662194
C	2.005870584	-1.803639330	-0.414676610
C	-1.361577777	-2.021332351	-1.064837315
H	-1.913861831	-2.960862277	-0.998025485
H	-0.774911780	-2.027325720	-1.986478899
C	0.803629006	-2.650823459	-0.034585703
H	0.676447964	-3.459712664	-0.755072676
H	1.021012377	-3.105475732	0.933007114

Bonds

Atom1	*Atom2*	*Length*
Ni	O	1.8315
Ni	N	2.0228
Ni	N	1.9068
Ni	N	1.9154
Ni	N	1.8364
O	C	1.2355
O	C	1.3309
N	C	1.3274
N	C	1.3982
O	C	1.2286
N	C	1.4009
N	C	1.3441
N	C	1.476
N	C	1.4717
N	C	1.4831
C	C	1.5185
C	H	1.0819
C	C	1.3945
C	C	1.3849
N	C	1.3934
N	C	1.3387
C	C	1.3977
C	C	1.3947
O	C	1.2267
C	H	1.0805
C	C	1.3962
C	C	1.3866
C	H	1.0822
C	C	1.3858
C	H	1.084
C	C	1.386
C	C	1.3885
C	H	1.0824
C	H	1.0834
C	C	1.3888
C	C	1.3885
C	C	1.5232
C	H	1.0835
C	C	1.3892
C	H	1.084
C	H	1.0841
C	H	1.0906
C	H	1.0911
C	H	1.0842

Angles

Atom1	*Atom2*	*Atom*
O	Ni	N
O	Ni	N
O	Ni	N
O	Ni	N
N	Ni	N
N	Ni	N
N	Ni	N
N	Ni	N
N	Ni	N
Ni	O	C
Ni	N	C
Ni	N	C
C	N	C
Ni	N	C
Ni	N	C
C	N	C
Ni	N	C
Ni	N	C
Ni	N	C
C	N	C
C	N	C
C	N	C
O	C	N
O	C	C
N	C	C
H	C	C
H	C	C
C	C	C
Ni	N	C
Ni	N	C
C	N	C
N	C	C
N	C	C
C	C	C
H	C	C
H	C	C
C	C	C
C	C	H
C	C	C
H	C	C
H	C	C
H	C	C
C	C	C

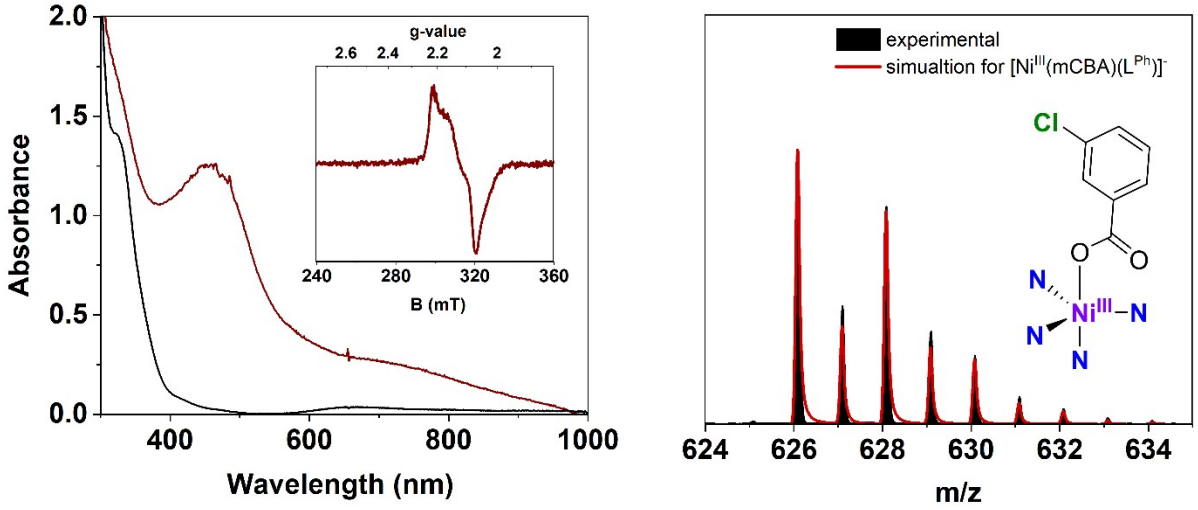

Figure S9. Left: Electronic absorption spectrum of **1[OAc]** (0.5 mM, black trace) and [Ni^{III}(*m*-CBA)(L^{Ph})]$^-$ (maroon trace, formed from the reaction between **1[OAc]** and *bis*(3-chlorobenzoyl)peroxide). Inset: X-Band EPR spectra of [Ni^{III}(*m*-CBA)(L^{Ph})]$^-$) (10.0 mM) in a frozen CH_3CN solution, collected at 77 K. Right: Negative mode ESI-MS spectrum obtained for [Ni^{III}(*m*-CBA)(L^{Ph})]$^-$. Black signal = experimental result, displaying *m/Z* = 626.0947. Maroon trace = simulation for [Ni(*m*-CBA)(L^{Ph})]$^-$, calc. *m/Z* for $C_{31}H_{25}ClN_4NiO_5$ = 626.0867.

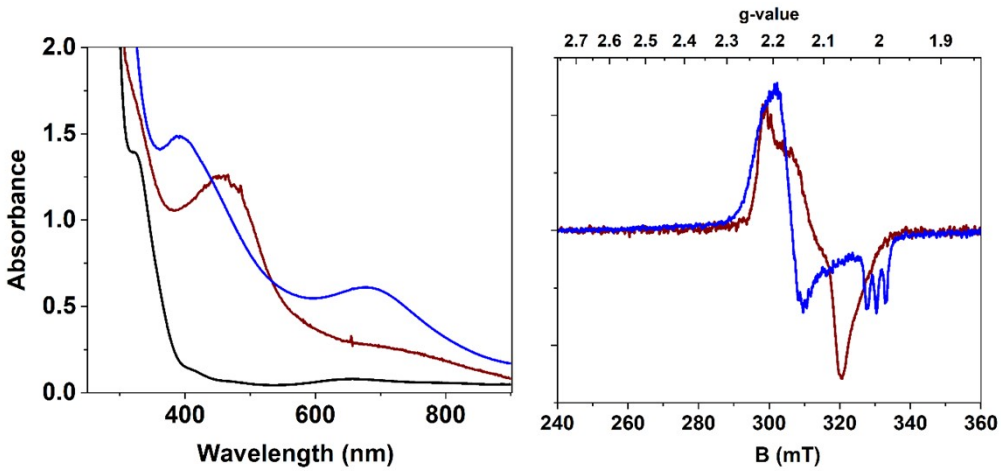

Figure S10. Left: Electronic absorption spectrum of **1[OAc]** (0.5 mM, black trace), **2[*m*-CBA]** (maroon trace) and **2** (blue trace). Right: X-Band EPR spectra of **2[*m*-CBA]**) (10.0 mM, maroon trace) and **2** (blue trace) in a frozen CH_3CN solution, collected at 77 K.

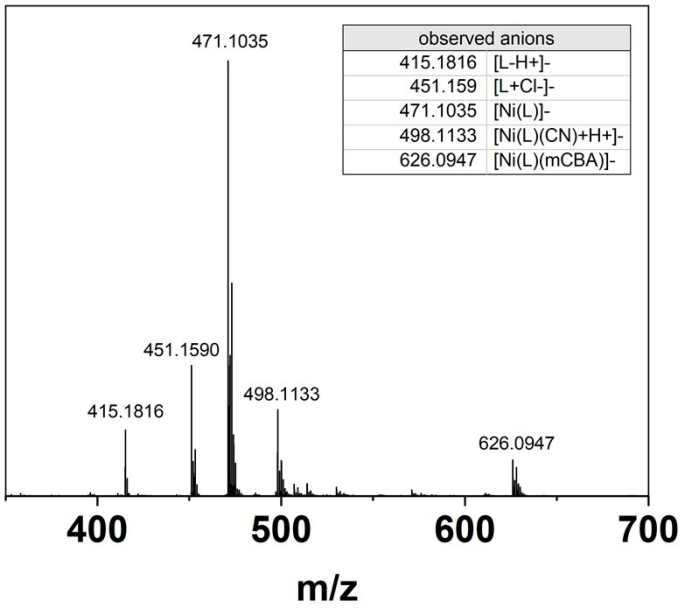

Figure S11. Negative mode ESI-MS spectrum obtained upon addition of 2.0 equiv. *bis*(3-chlorobenzoyl)peroxide to **1[OAc]** at -40 °C in CH_3CN.

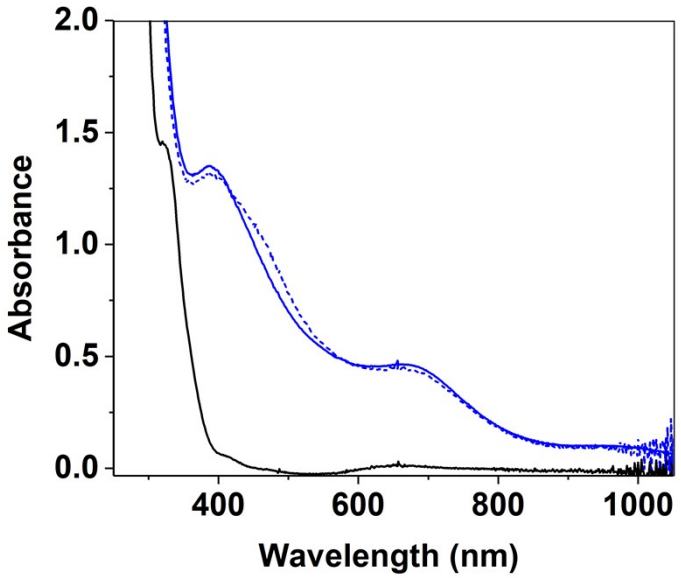

Figure S12. Electronic absorption spectrum of **1[OAc]** (0.50 mM, Black trace), **2** generated with 1.0 equiv. *m*-CPBA (solid blue trace) and 1.0 equiv. peroxybenzoic acid (dashed blue trace) in CH_3CN at -40 °C.

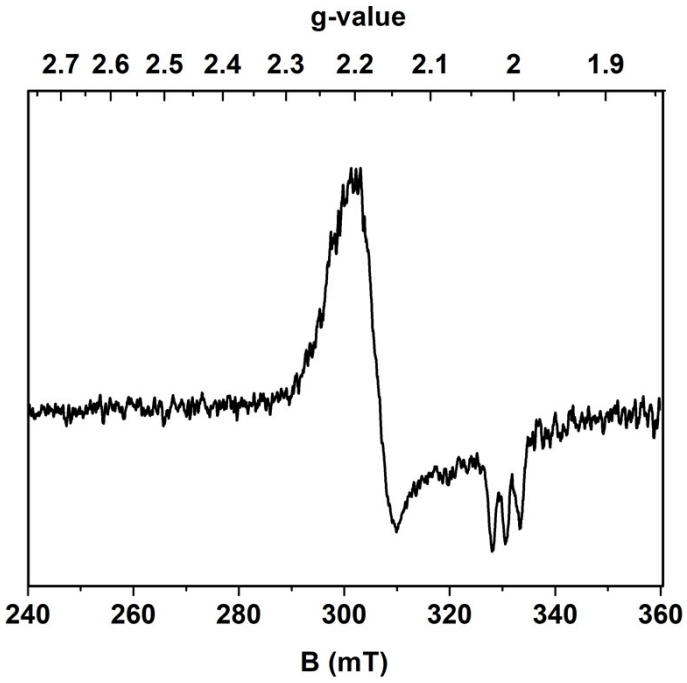

Figure S13. X-Band EPR spectrum of **2**, generated upon addition of perbenzoic acid (1.0 equiv.) to **1[OAc]** (10.0 mM) at -40 °C in CH_3CN. EPR spectrum collected at 77 K, 2.02 mW microwave power and 0.3 mT modulation amplitude.

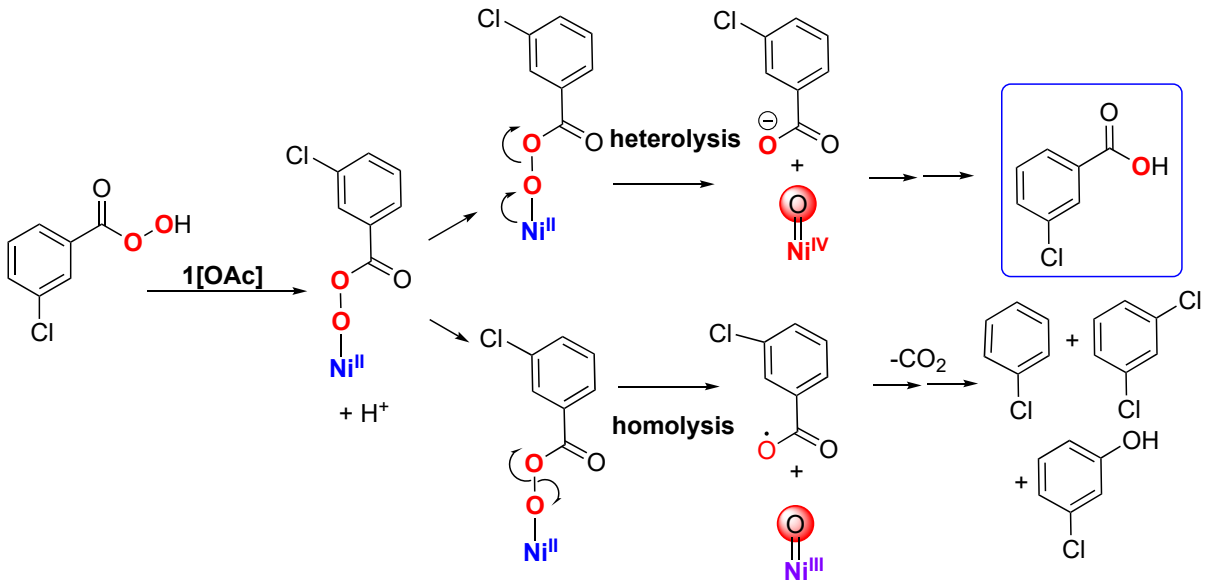

Scheme S1. Possible decay pathways of *m*-CPBA upon reaction with Ni^{II}.

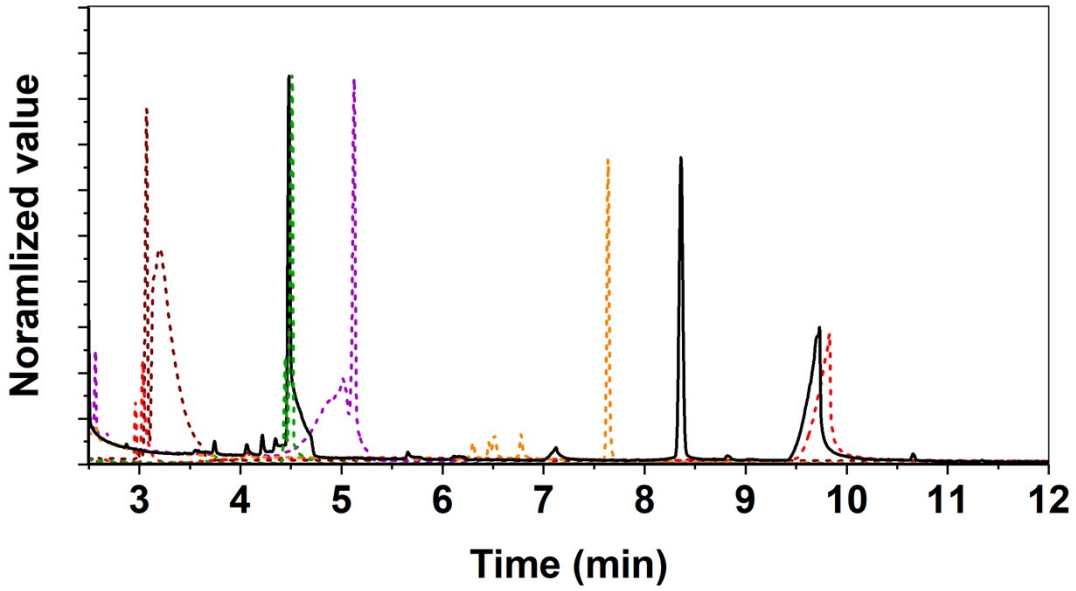

Figure S14. GC-FID overlay spectrum of a post reaction mixture of **1[OAc]** with *m*-CPBA (1.0 equiv., black solid trace) and pristine samples of: chlorobenzene (3.1 min, maroon dashed trace), aniline (4.5 min, green dashed trace), 1,3-dichlorobenzene (5.1 min. purple dashed trace), 3-chlorophenol (7.6 min, orange dashed trace) and 3-chlorobenzoic acid (9.8 min, red dashed trace) in CH_3CN.

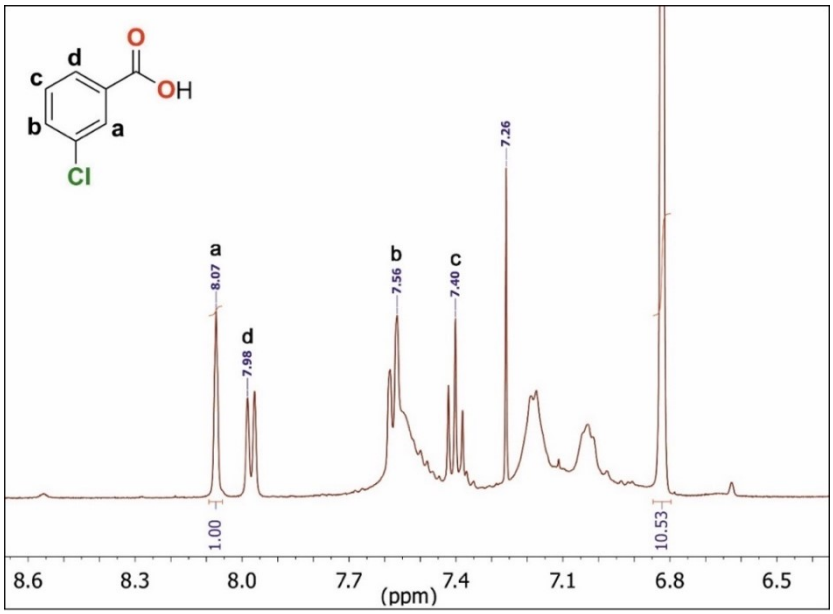

Figure S15. ^{1}H NMR of the organic extract of **1[OAc]** (10.0 mM) with *m*-CPBA (1.0 equiv.) in $CDCl_3$ at 25 °C.

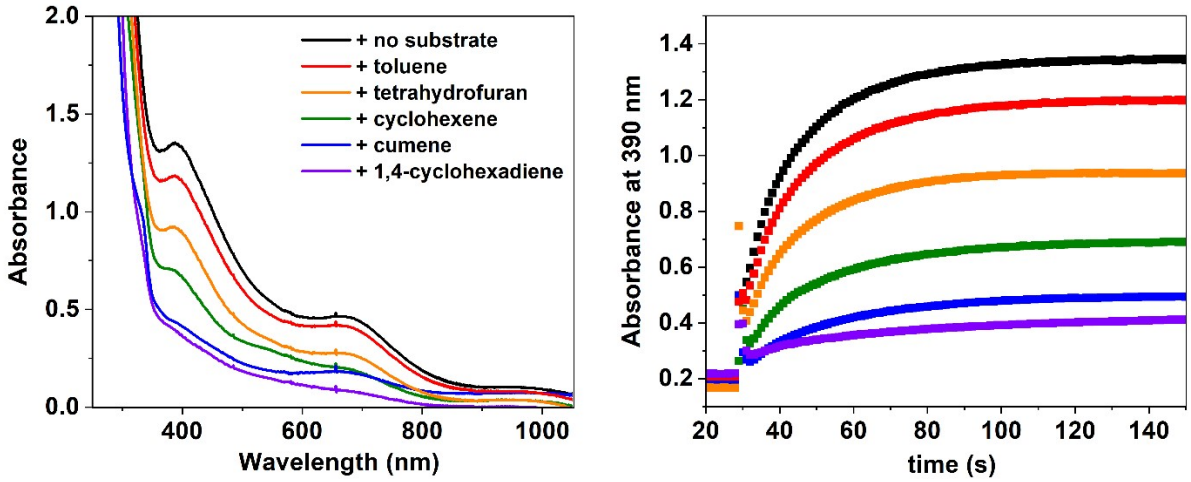

Figure S16. Addition of no substrate, then 100 µl toluene, tetrahydrofuran, cyclohexene, cumene, and 1,4-cyclohexadiene to **1[OAc]** prior to adding *m*-CPBA at -40 °C in CH_3CN.

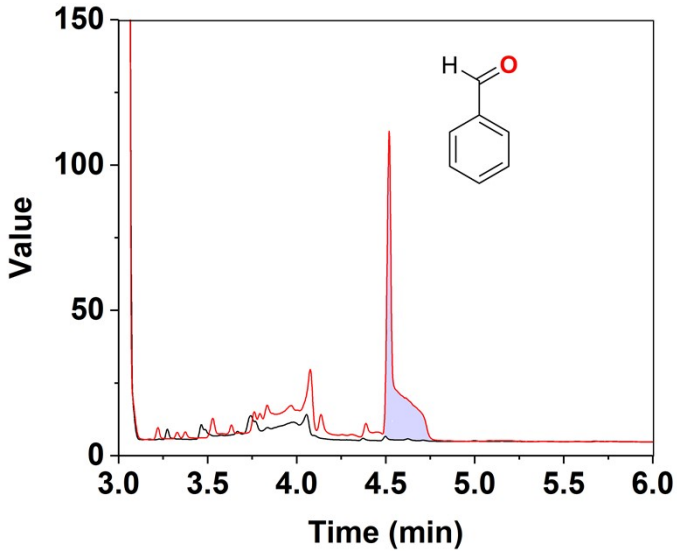

Figure S17. GC-FID of a post reaction mixture for the reaction of **1[OAc]** with *m*-CPBA in the presence of toluene (940 equiv., red trace) in CH_3CN.

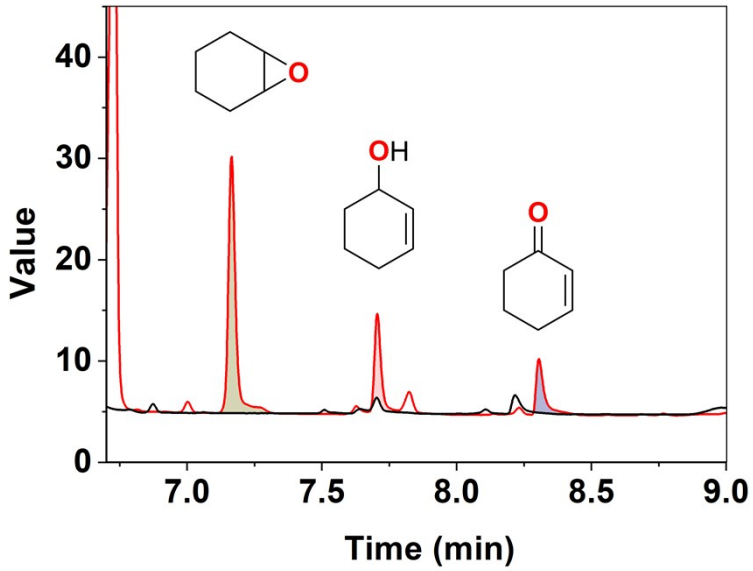

Figure S18. GC-FID of a post reaction mixture for the reaction of **1[OAc]** with *m*-CPBA in the presence of cyclohexene (980 equiv., red trace).

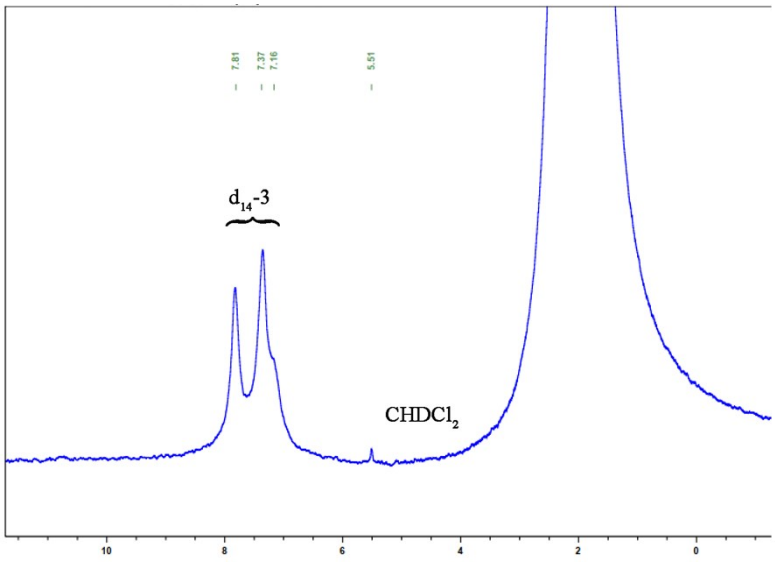

Figure S19. ^{1}H NMR (600 MHz) of a post reaction mixture **D_{15}-1[OAc]** with *m*CPBA in CD_3CN.

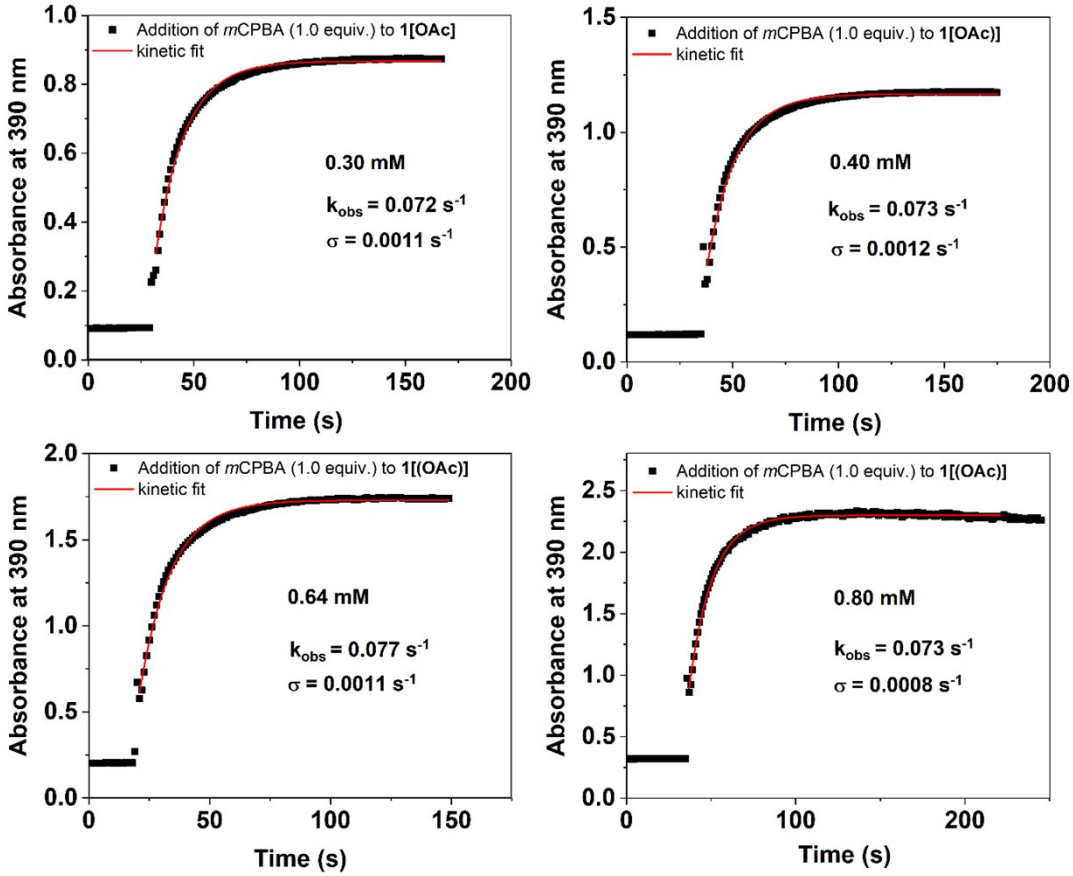

Figure S20. Kinetic traces, monitoring the formation of **2** (λ = 390 nm) at different concentrations of **1[OAc]** from its reaction with *m*CPBA in CH_3CN at -40 °C.

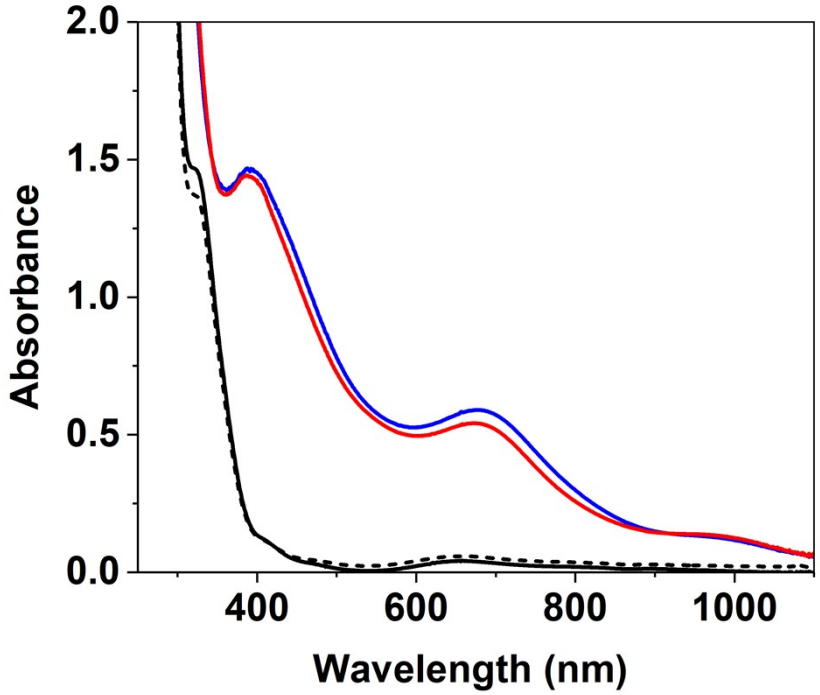

Figure S21. Electronic absorption spectrum of **1[OAc]** (0.50 mM, black solid trace) and **1[OAc]-D$_{15}$** (0.50 mM, black dashed trace), **2** (0.50 mM, blue trace) and **2-D$_{15}$** in CH_3CN at -40 °C.

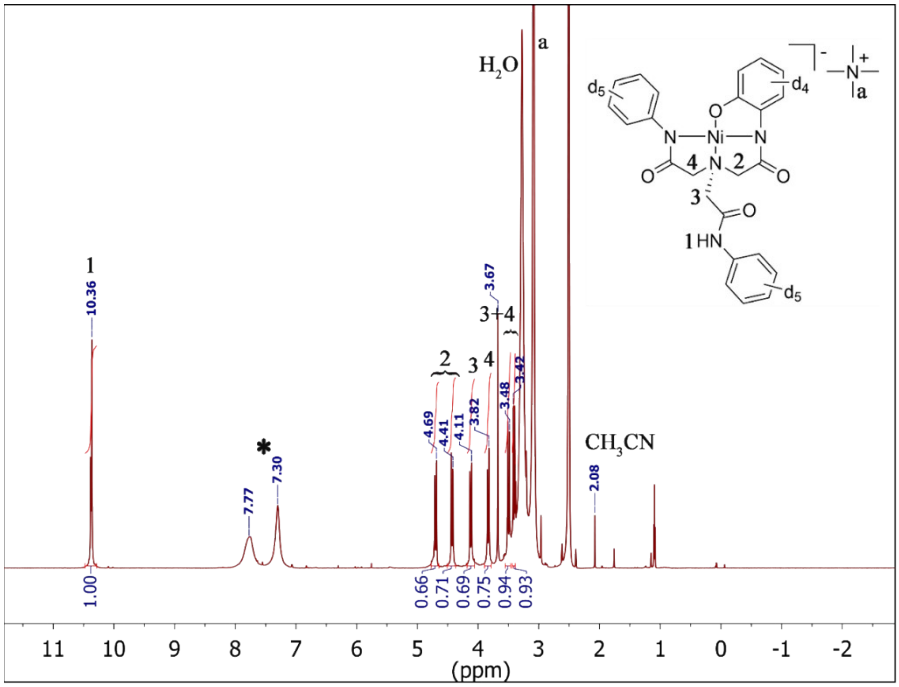

Figure S22. ^{1}H NMR (600 MHz) of a post reaction mixture **1[OAc]-D$_{15}$** with *m*CPBA after Et_2O wash to remove excess *m*-CBA in [D_6]-DMSO. * Unidentified impurity.

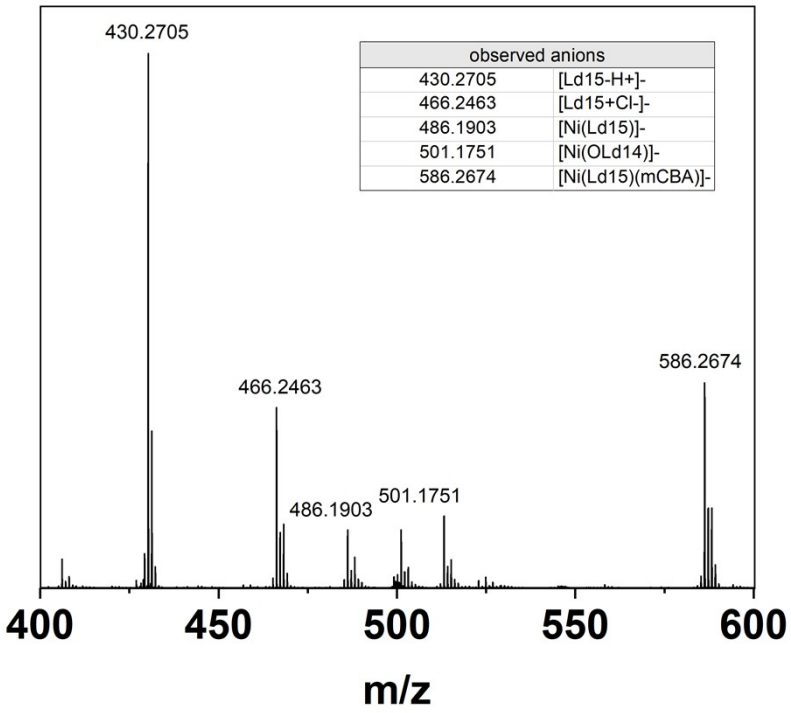

Figure S23. Negative mode ESI-MS spectrum obtained upon addition of 1.0 equiv. *m*CPBA to **1[OAc]-D_{15}** at -40 °C in CH_3CN.

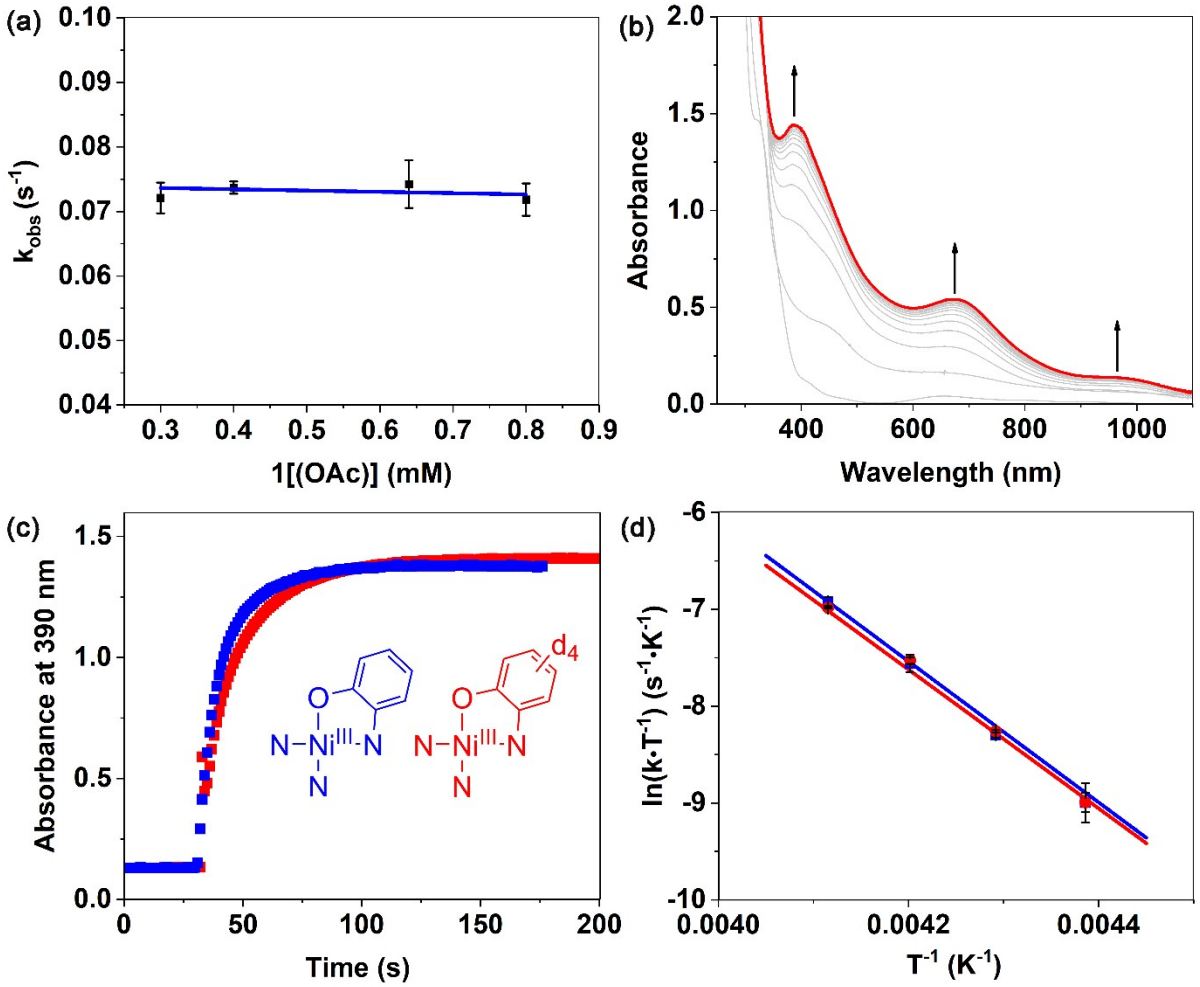

Figure S24. (a) Rate of formation of **2** upon addition of *m*-CPBA (1.0 equiv.) to **1[OAc]** at different concentrations of **1[OAc]** in CH_3CN at -40 °C. (b) Electronic absorption spectrum showing incremental changes in absorbance (grey traces) upon addition of *m*-CPBA to **1[OAc]-D_{15}** (0.50 mM) forming **2-D_{14}** (0.50 mM, red trace) in CH_3CN at -40 °C. (c) Kinetic traces monitoring changes the electronic absorption spectrum at λ = 390 nm, upon addition of *m*-CPBA to **1[OAc]** (0.50 mM, blue trace) and **1[OAc]-D_{15}** (0.50 mM, red trace) in CH_3CN at -40 °C. (d) Eyring plot (ln(kT^{-1}) *versus* T^{-1}) for the conversion of **1[OAc]** to **2** (blue line, Slope = 7280 ± 340) and **1[OAc]-D_{15}** to **2-D_{14}** (red line, Slope = 7170 ± 250).

Table S9. First Order rate constants upon addition of *m*CPBA (1.0 equiv.) to **1[OAc]** and **1[OAc]-D_{15}** in CH_3CN at -40 °C.

1[OAc]				**D_{15}-1[OAc]**			
T (K)	T^{-1} (K^{-1})	k_{obs} (s^{-1})	ln(k_{obs} x K^{-1})	T (K)	T^{-1} (K^{-1})	k_{obs} (s^{-1})	ln(k_{obs} x K^{-1})
228	0.0044	0.028	-9.00	228	0.0044	0.028	-9.00
233	0.0043	0.060	-8.26	233	0.0043	0.058	-8.30
238	0.0042	0.128	-7.53	238	0.0042	0.124	-7.56
243	0.0041	0.227	-6.98	243	0.0041	0.239	-6.92

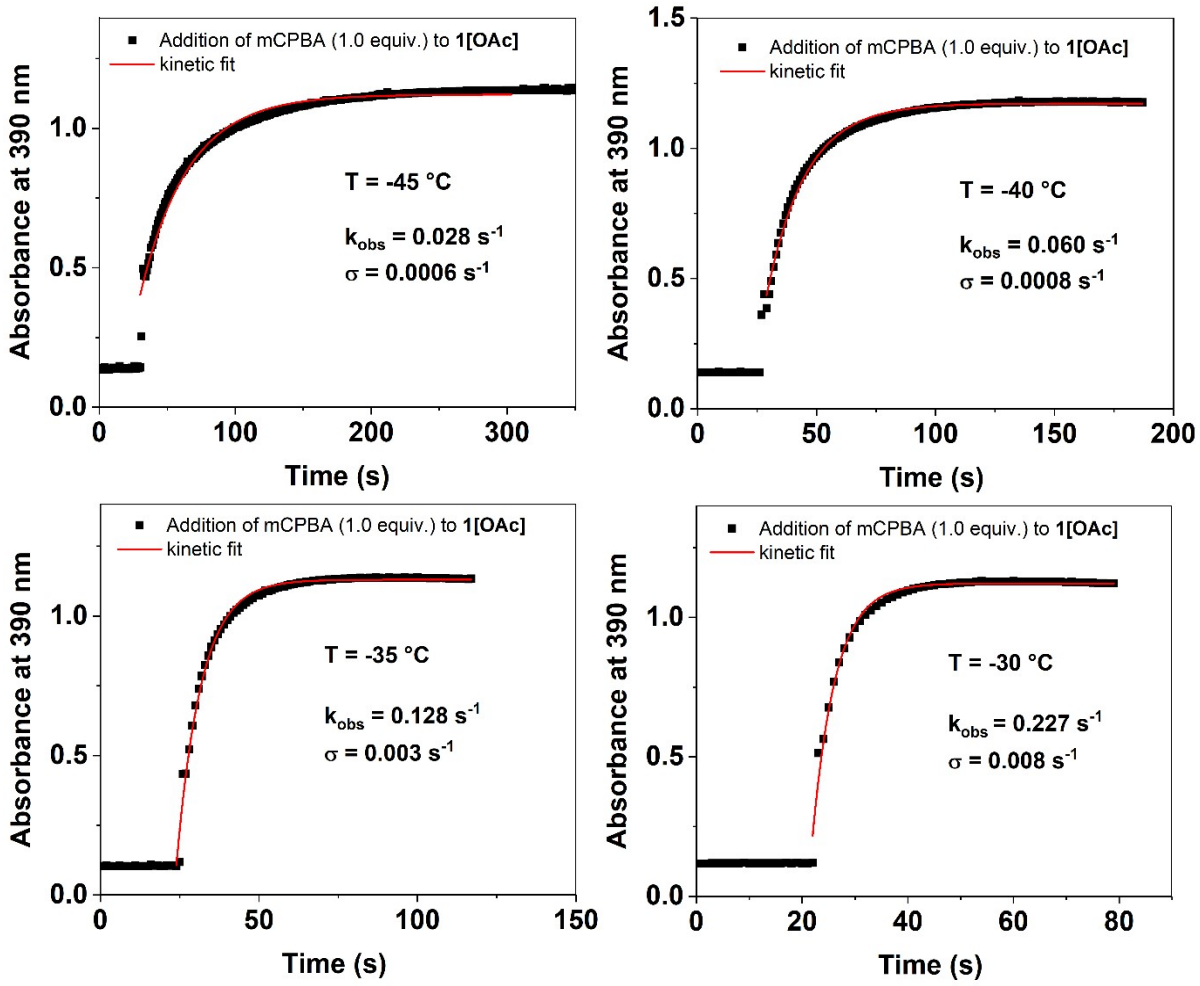

Figure S25. Kinetic traces, monitoring the formation of **2** (0.40 mM, λ = 390 nm) at different temperatures (228 – 243 K) in CH_3CN.

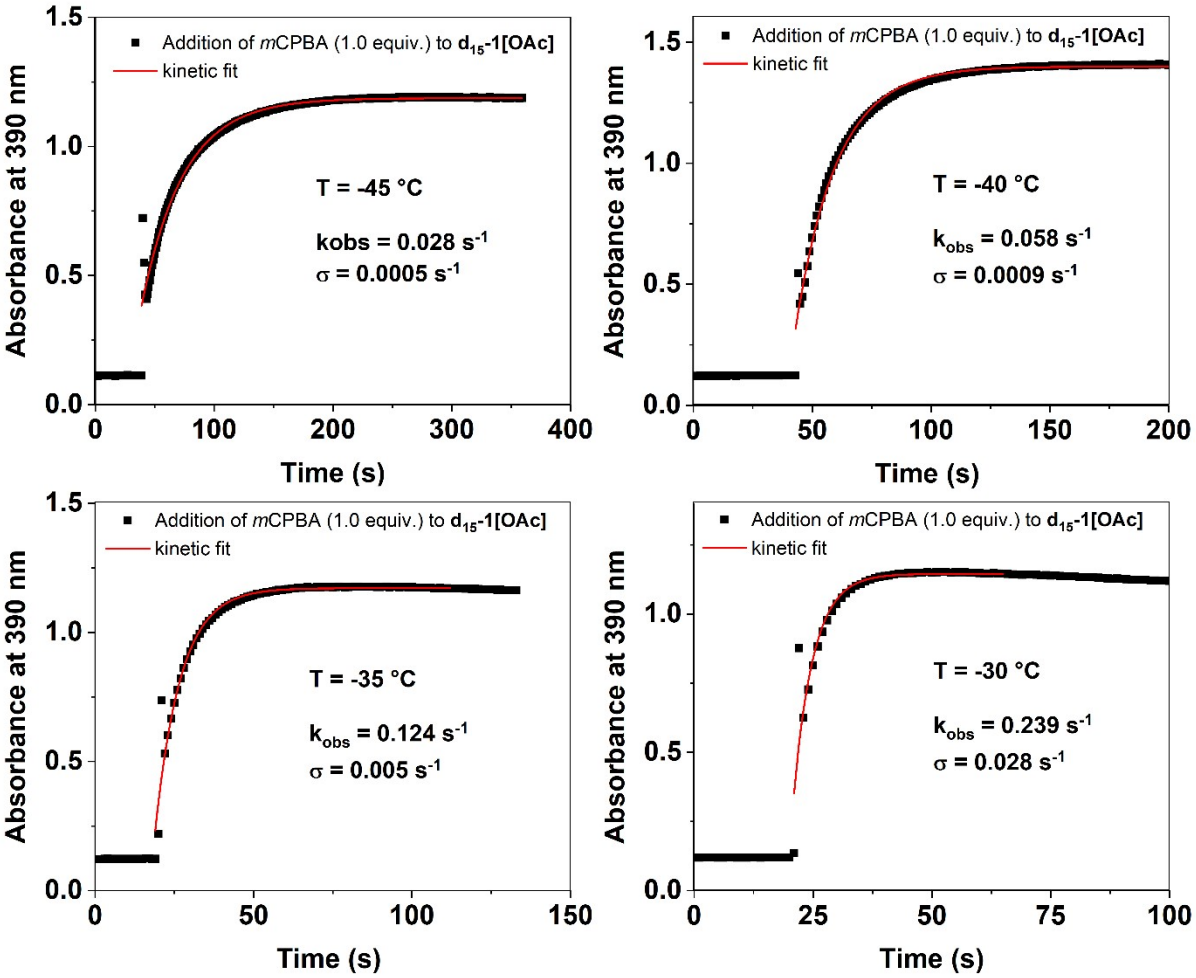

Figure S26. Kinetic traces, monitoring the formation of **2-D_{14}** (0.40 mM, λ = 390 nm) at different temperatures (228 – 243 K) in CH_3CN.

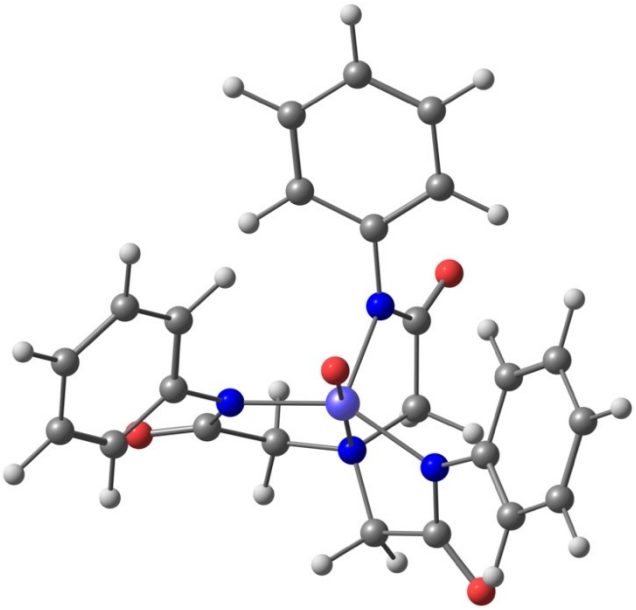

Figure S27. Optimized molecular structure of **[NiO(NTA)]**$^{-}$ (S = 0). Final single point energy: -2974.803425314289 a.u.; final Gibbs free energy: -2974.44079299 a.u.

Table S10. Atomic coordinates for optimized structure of **[NiO(NTA)]**$^{-}$ (S = 0).

Ni	0.000000000	0.000000000	0.000000000
O	3.421209281	-1.736087947	-1.005488997
O	-3.033542660	-1.387853225	-2.090151660
O	-0.644092737	-2.173763027	3.351776745
O	0.000000000	1.757212754	0.000000000
N	-0.085040403	-1.917715472	-0.180670523
N	1.845491114	-0.131249825	-0.491219128
N	-1.823924279	-0.081579269	-0.609215357
N	0.000000000	-0.452170576	1.955204527
C	1.286825434	-2.443198215	-0.258164563
H	1.338956243	-3.282380466	-0.953387143
H	1.576272658	-2.812702797	0.726979761
C	2.298878380	-1.385853033	-0.648416842
C	2.646253646	0.964882583	-0.856356481
C	2.751861786	2.059707420	-0.000556502
H	2.239952898	2.034596165	0.951818417
C	3.498664465	3.170621175	-0.365440132
H	3.565461264	4.012813518	0.313678354
C	4.156507344	3.204816743	-1.585838616
H	4.742225500	4.071125962	-1.869440570
C	4.050576507	2.117371783	-2.444907342
H	4.551783604	2.134805645	-3.406076344
C	3.300064778	1.008964648	-2.089314716
H	3.213816104	0.169224774	-2.765537221
C	-0.865283057	-2.105530777	-1.409839721
H	-1.219781220	-3.134533208	-1.500949195
H	-0.228310187	-1.881928240	-2.269282444
C	-2.041964493	-1.141185314	-1.408558053
C	-2.747216968	0.960359684	-0.462008529
C	-3.571951851	1.408504473	-1.496973712

H	-3.532032082	0.921009404	-2.459601978
C	-4.437952161	2.470911000	-1.286190705
H	-5.069415648	2.807820314	-2.100548145
C	-4.498409147	3.107809929	-0.053825717
H	-5.177340288	3.937635752	0.101877235
C	-3.673611834	2.671466439	0.974296958
H	-3.700700855	3.159776232	1.941691095
C	-2.808118614	1.609895154	0.772580068
H	-2.157852932	1.270055052	1.567368800
C	-0.802826848	-2.451910179	0.991417028
H	-0.562790267	-3.507140627	1.130331309
H	-1.876266948	-2.365293460	0.818580125
C	-0.463292802	-1.662175962	2.241685294
C	0.382086812	0.421158327	2.983175806
C	-0.559572352	1.017506214	3.820928583
H	-1.606660923	0.766706981	3.701823870
C	-0.160941653	1.914140142	4.800171448
H	-0.905112721	2.370142623	5.443131631
C	1.182074269	2.231607874	4.957946531
H	1.490608845	2.936713407	5.720612198
C	2.125638948	1.634705504	4.132926119
H	3.177423195	1.869660122	4.250123704
C	1.729005813	0.734160431	3.155749192
H	2.459798170	0.261603553	2.510617619

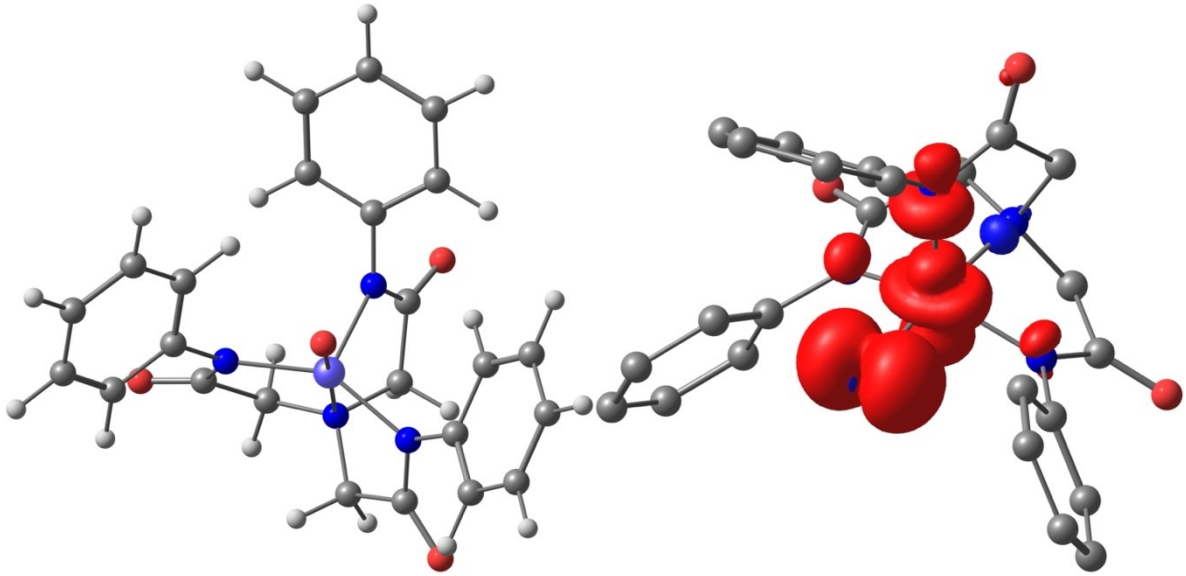

Figure S28. Optimized molecular structure of **[NiO(NTA)]**$^{-}$ (S = 1, left) and electron spin-density plot (right; H atoms omitted for clarity; isosurface value at 0.005). Final single point energy: -2974.804993430248 a.u.; final Gibbs free energy (293.15 K): -2974.44403605 a.u.; final Gibbs free energy (298.15 K): -2974.44537061 a.u.; final entropy term (298.15 K): 0.08508531 a.u.

Table S11. Atomic coordinates for optimized structure of **[NiO(NTA)]**$^{-}$ (S = 1).

Ni	0.000000000	0.000000000	0.000000000
O	-1.747995790	-3.424747743	-0.987686377
O	-1.370280846	3.030051818	-2.108757680
O	-2.204182234	0.652529871	3.332891508
O	1.731721126	0.000000000	0.000000000
N	-1.919342062	0.089606856	-0.194983646
N	-0.141562510	-1.848593363	-0.481606014
N	-0.084716182	1.823333670	-0.609341493
N	-0.474420207	0.000000000	1.950717909
C	-2.451620766	-1.279994943	-0.267093270
H	-3.284634260	-1.332027617	-0.969688759
H	-2.831919548	-1.560265399	0.716528960
C	-1.396374077	-2.299617075	-0.640515955
C	0.953128545	-2.656375845	-0.835716282
C	2.041600170	-2.765372570	0.027472763
H	2.014317454	-2.248529892	0.977131321
C	3.149650361	-3.521083970	-0.327148517
H	3.987036518	-3.590702626	0.357588677
C	3.187497244	-4.183880463	-1.544929394
H	4.051832701	-4.776248780	-1.820575868
C	2.106557351	-4.074173539	-2.411540911
H	2.126885890	-4.579025324	-3.370722223
C	1.000821978	-3.315073442	-2.065757632
H	0.165768944	-3.226050750	-2.747485024
C	-2.097498509	0.863095369	-1.429760785
H	-3.125907026	1.216601149	-1.530776299

H	-1.866132959	0.222016232	-2.283996701
C	-1.133460280	2.039175143	-1.422813934
C	0.952443538	2.751214486	-0.452380621
C	1.436321042	3.541256810	-1.497588942
H	0.983317857	3.468107262	-2.475287850
C	2.490105237	4.415751577	-1.278212313
H	2.856012803	5.020446681	-2.100283562
C	3.081923433	4.517444622	-0.026323850
H	3.905535326	5.202268640	0.136470265
C	2.609619507	3.726556113	1.012685088
H	3.063461808	3.786882718	1.995213535
C	1.556495276	2.853070035	0.801770009
H	1.188516145	2.227703030	1.603902833
C	-2.459219302	0.815581398	0.969615572
H	-3.517516383	0.583763224	1.098694184
H	-2.362160078	1.887736939	0.795121424
C	-1.683813939	0.470542461	2.227134702
C	0.384143695	-0.397585044	2.985732112
C	0.987525514	0.532543590	3.831131824
H	0.754799129	1.583774037	3.712547979
C	1.868766232	0.117563455	4.817547206
H	2.330695294	0.852990775	5.466286047
C	2.163165555	-1.230712121	4.975223699
H	2.856266338	-1.552143576	5.743530975
C	1.558658825	-2.162809784	4.142791337
H	1.775575687	-3.218475173	4.259733604
C	0.673547639	-1.749748129	3.158310524
H	0.195709881	-2.471370343	2.506799367

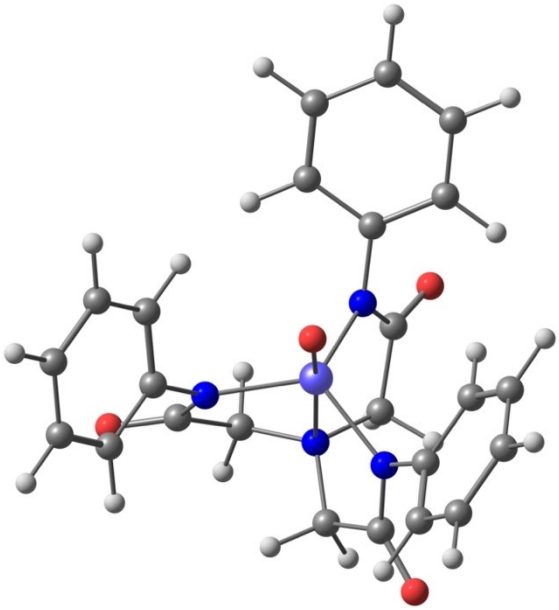

Figure S29. Optimized molecular structure of **[NiO(NTA)]**$^{-}$ (S = 2). Final single point energy: -2974.791987243068 a.u.; final Gibbs free energy: -2974.43312187 a.u.

Table S12. Atomic coordinates for optimized structure of **[NiO(NTA)]**$^{-}$ (S = 2).

Ni	0.000000000	0.000000000	0.000000000
O	1.138493387	-3.416222131	-1.839403623
O	1.960077028	2.710220959	-2.287581652
O	-3.671293229	0.497489465	-1.570733059
O	0.449825820	0.151550674	1.760537439
N	-0.199567963	-0.122762302	-2.156631639
N	0.879905852	-1.701812375	-0.326466591
N	0.861806066	1.663998181	-0.551991940
N	-1.911741085	0.024161061	-0.168150068
C	-0.190068598	-1.543066121	-2.460192396
H	0.115237694	-1.743865991	-3.491200393
H	-1.200994185	-1.938530451	-2.331750586
C	0.707141675	-2.312541902	-1.509648100
C	1.687897877	-2.309206227	0.649458800
C	1.138452459	-2.662767237	1.879941898
H	0.083121566	-2.490760248	2.051671019
C	1.932494428	-3.224352206	2.868871141
H	1.491210836	-3.491543036	3.822115505
C	3.283464573	-3.443206089	2.640609417
H	3.904461908	-3.881074144	3.413028008
C	3.835700754	-3.092756774	1.413850884
H	4.891272385	-3.255590270	1.228594795
C	3.046712778	-2.528497367	0.425192325
H	3.476150893	-2.245701989	-0.528006352
C	0.953942896	0.589928424	-2.680758674
H	0.800061209	0.925225887	-3.710729014
H	1.815981579	-0.082535759	-2.676743657

C	1.311625828	1.780243051	-1.810186282
C	1.194487215	2.596290284	0.435827165
C	2.499275692	3.061322511	0.618701268
H	3.278835824	2.730381660	-0.053832558
C	2.789630589	3.930544565	1.655974938
H	3.807362349	4.279703060	1.788679154
C	1.793052984	4.347671437	2.531672006
H	2.028868698	5.025115102	3.343643061
C	0.496292524	3.886752930	2.356993450
H	-0.290145335	4.201567264	3.032992745
C	0.197988030	3.020468123	1.316540623
H	-0.813686325	2.659112048	1.173794780
C	-1.462351399	0.530723893	-2.460944677
H	-1.890917001	0.181912641	-3.404769418
H	-1.290596331	1.606000731	-2.554603603
C	-2.473974215	0.340609557	-1.348292862
C	-2.728416332	-0.150236226	0.965147160
C	-3.450152529	0.911509304	1.505770574
H	-3.406044744	1.880173443	1.023241768
C	-4.204739595	0.727892001	2.653286149
H	-4.759019785	1.561852666	3.068237730
C	-4.247193283	-0.513794163	3.275595403
H	-4.834107372	-0.652489850	4.175682761
C	-3.530933611	-1.573987769	2.737399454
H	-3.556658777	-2.546591571	3.214966191
C	-2.776713372	-1.393981059	1.587756421
H	-2.213488685	-2.215315436	1.160319356

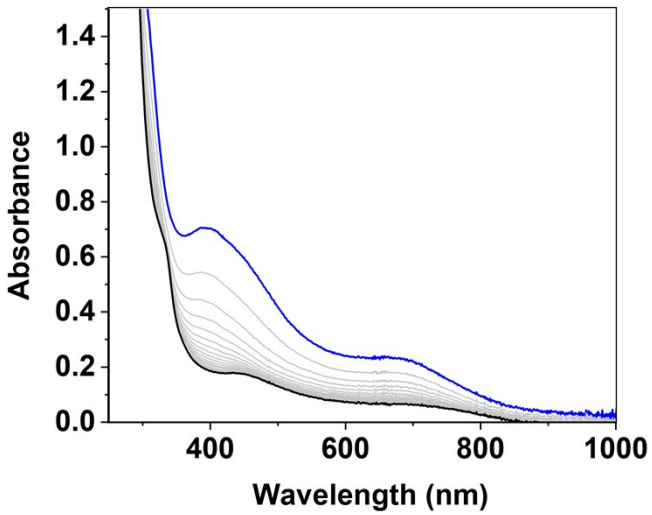

Figure S30. Electronic absorption spectrum of **2** (0.3 mM, blue trace) upon addition of CHD (100 equiv.) in CH_3CN at -40 °C. Grey traces showing incremental changes in the electronic absorption spectrum of **2**. Black trace showing the final spectrum after 1200 s.

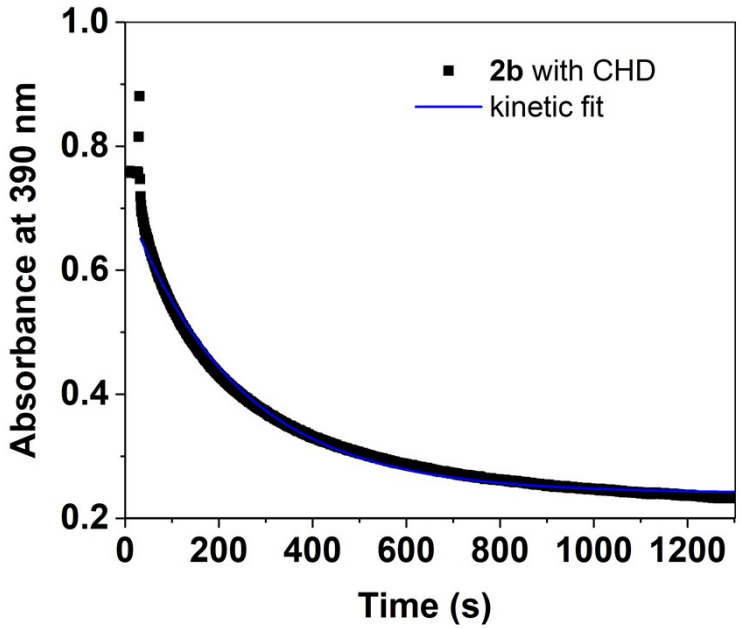

Figure S31. Kinetic trace, monitoring changes in the electronic absorption spectrum of **2** upon addition of CHD (100 equiv.) in CH_3CN at -40 °C.

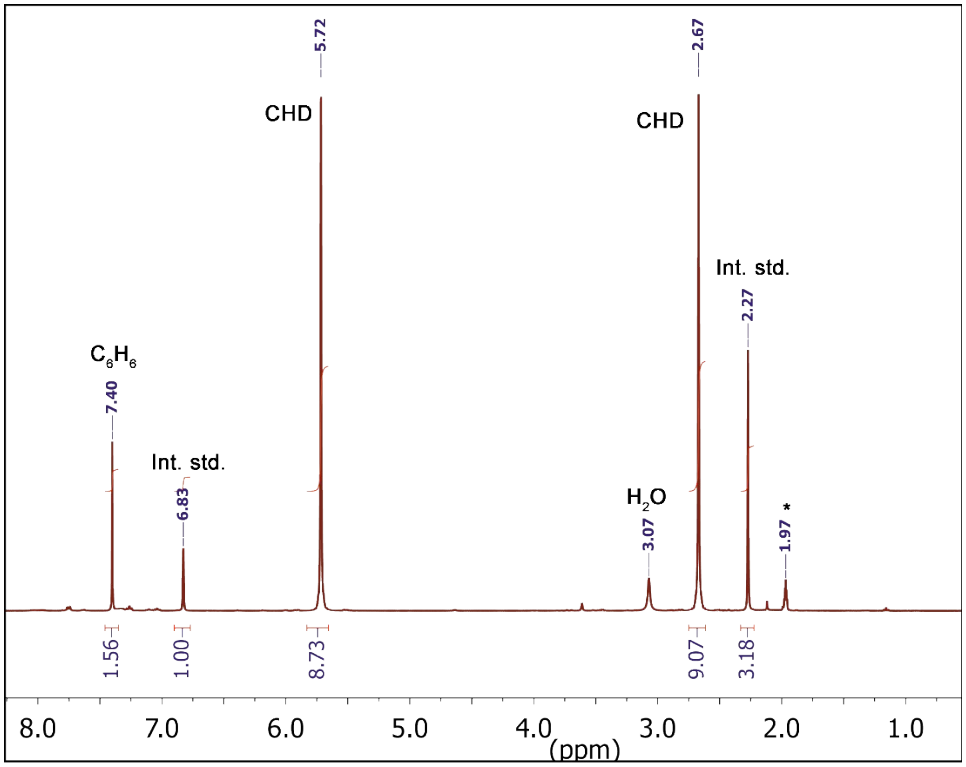

Figure S32. ^{1}H NMR spectrum for the reaction of **2** with CHD (35 equiv.) in CD_3CN. Reaction carried out at -40 °C. *residual solvent peak.

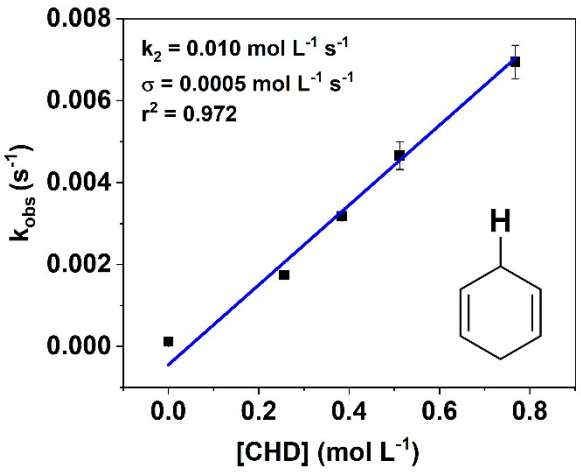

Figure S33. Plots of k_{obs} *vs*. [substrate] for the reactions of **2** with 1,4-cyclohexadiene at -40 °C in CH_3CN.

References

1. S. Stoll and A. Schweiger, *J. Mag. Reson.*, 2006, **178**, 42-55.
2. B. Ravel and M. Newville, *J. Synch. Rad.*, 2005, **12**, 537-541.
3. F. Neese, *Wiley Interdisciplinary Reviews: Computational Molecular Science*, 2012, **2**, 73-78.
4. F. Weigend and R. Ahlrichs, *Phys. Chem. Chem. Phys.*, 2005, **7**, 3297-3305.
5. D. A. Pantazis and F. Neese, *WIREs Computational Molecular Science*, 2014, **4**, 363-374.
6. C. v. Wüllen, *J. Chem. Phys.,* 1998, **109**, 392-399.
7. E. van Lenthe, E. J. Baerends and J. G. Snijders, *J. Chem. Phys.*, 1993, **99**, 4597-4610.
8. S. Grimme, *J. Comput. Chem.*, 2006, **27**, 1787-1799.
9. S. Grimme, J. Antony, S. Ehrlich and H. Krieg, *J. Chem. Phys.*, 2010, **132**, 154104.
10. T. Lu and F. Chen, *J. Comput. Chem.*, 2012, **33**, 580-592.
11. D. G. Harman, A. Ramachandran, M. Gracanin and S. J. Blanksby, *J. Org. Chem.*, 2006, **71**, 7996-8005.
12. J. M. Rowland, G. J. Ibanez, M. M. Olmstead, M. Ruf and P. K. Mascharak, *Acta Cryst. E*, 2001, **57**, o1001-o1003.
13. W.-Y. Yu, W. N. Sit, Z. Zhou and A. S.-C. Chan, *Org. Lett.*, 2009, **11**, 3174-3177.
14. *Slovenia Pat.,* EP3511295, 2019.
15. P. Heim, G. Spedalotto, M. Lovisari, R, Gericke, J. O'Brien, E. R. Farquhar, A. R. McDonald, *Chem. Eur. J.*, 2023, DOI: 10.1002/chem.202203840.